Effect of material and geometric parameters on deformations near the notch-tip of a dynamically loaded prenotched plate

R.C. BATRA and R.R. GUMMALLA
Department of Engineering Science and Mechanics, MC.219, Virginia Polytechnic Institute and State University, Blacksburg, VA 24061, U.S.A. e-mail: rbatra@vt.edu

Abstract. We analyze plane strain thermomechanical deformations of a prenotched rectangular plate impacted on one side by a prismatic body of rectangular cross-section and moving parallel to the axis of the notch. Both the plate and the projectile are made of the same material. Strain hardening, strain-rate hardening and thermal softening characteristics of the material are modeled by the Johnson–Cook relation. The effect of different material parameters, notch-tip radius, impact speed and the length of the projectile on the maximum tensile principal stress and the initiation and propagation of adiabatic shear bands at the notch-tip is analyzed. It is found that for high impact speeds or enhanced thermal softening, two shear bands, one at $-10°$ to the notch ligament and the other at $-128°$ to it, propagate from the notch tip. Otherwise, only one shear band nearly parallel to the notch-ligament initiates at the notch-tip. The notch-tip distortion for high strength materials is quite different from that for low strength materials. The maximum tensile principal stress occurs at a point on the upper surface of the notch-tip and for every set of values of material parameters and impact speeds studied equals about 2.3 times the yield stress of the material in a quasistatic simple tension or compression test. We assume that the brittle failure occurs when the maximum tensile principal stress equals twice the yield stress of the material in a quasistatic simple tension test and a shear band initiates when the effective plastic strain at a point equals 0.5. The effect of material and geometric parameters on the time of initiation of each failure mode is computed. It is found that for low impact speeds (< 30 m/s) a material will fail due to the maximum tensile principal stress exceeding its limiting value, and at high impact speeds due to the initiation of a shear band at the notch-tip. Results are also computed for a C-300 steel with material parameters given by Zhou et al. For an impact speed of 50 m/s, the shear band speed and the maximum effective plastic strain-rate before a material point melts are found to be 350 m/s and 5×10^7/s respectively.

Key words: Failure-mode transition, shear bands, thermoviscoplasticity, numerical simulations.

1. Introduction

Kalthoff (1987) and Kalthoff and Winkler (1987) have experimentally studied the deformations near the notch tip in a prenotched rectangular plate made of a maraging steel and impacted on the notched side by a cylindrical projectile moving parallel to the axis of the notch. They obtained essentially identical results for both single notched and double notched plates. For impact speeds V_0 below a critical value V_c, a crack developed at a point on the notch surface and propagated into the plate at about 70° to the notch-axis. However, for impact speeds greater than V_c a shear band developed at the notch tip and propagated at an angle of $-10°$ to $-15°$ to the notch-axis. They postulated that the maximum effective plastic strain-rate at the notch-tip is proportional to $V_0/\sqrt{r_0}$ where r_0 is the radius of the notch-tip. Mason et al. (1994) and Zhou et al. (1996a) also used an experimental set-up similar to that of Kalthoff (e.g. see Figure 1) and found that no failure ensued at low impact speeds but at high speeds of
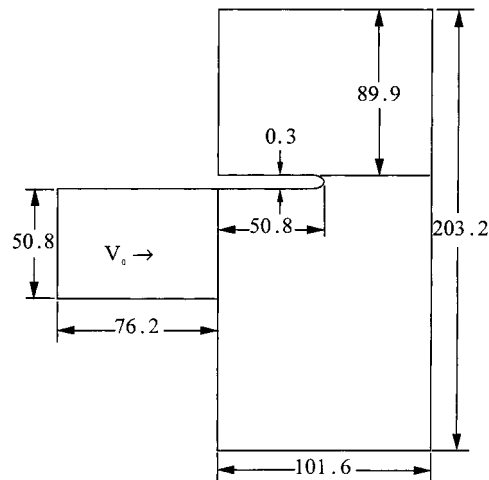
All dimensions are in mm (Sketch not to scale)

Figure 1. A schematic sketch of the problem studied.

impact a shear band initiating from the notch-tip propagated nearly parallel to the notch-axis, got arrested and a crack ensued from the shear band tip. They attributed the difference in their and Kalthoff's experimental results to different values of material parameters. We note that Kalthoff listed only the Rockwell hardness number for the steel tested and did not provide stress-strain curves. Mason et al. (1994a) have given the shear stress vs. the logarithmic shear strain curve for the C-300 maraging steel, and Zhou et al. (1996b) have evaluated the material parameters by curve fitting.

Needleman and Tvergaard (1995), Zhou et al. (1996b) and Batra and Nechitailo (1997) have used the finite element method to simulate Kalthoff's experiment and employed different constitutive relations to model the thermoviscoplastic response of the material. Each of these investigations assumed that a plane strain state of deformation prevails in the plate. Batra and Nechitailo (1997) also modeled the deformations of the projectile. Needleman and Tvergaard (1995) enforced essential boundary conditions at the impacted face with the maximum value of the prescribed velocity equal to one-half of the initial velocity of the projectile. However, Zhou et al. (1996b) presumed that the maximum value of the prescribed velocity equals the initial velocity of the striker. Needleman and Tvergaard (1995) accounted for the softening of the material due to the evolution of the porosity and also due to the temperature rise but the other two investigations considered thermal softening only. These works did not study the effect of different material parameters on the deformations of the plate material adjacent to the notch-tip. Here we model the thermoviscoplastic response of the material by the Johnson–Cook (1983) relation and analyze the effect of the change in the value of each material parameter on the deformations of the plate material close to the notch-tip. In each case, the deformations of the projectile are also considered and both the plate and the striker are taken to be made of the same material. The effect of the impact speed, notch-tip radius, and the length of the projectile on deformations of the plate are also investigated. By assuming that the brittle failure ensues when the maximum tensile principal stress at a point equals twice the yield stress of the material in a quasistatic simple tension or compression test and a shear band

DIMENSIONS ARE IN MM.
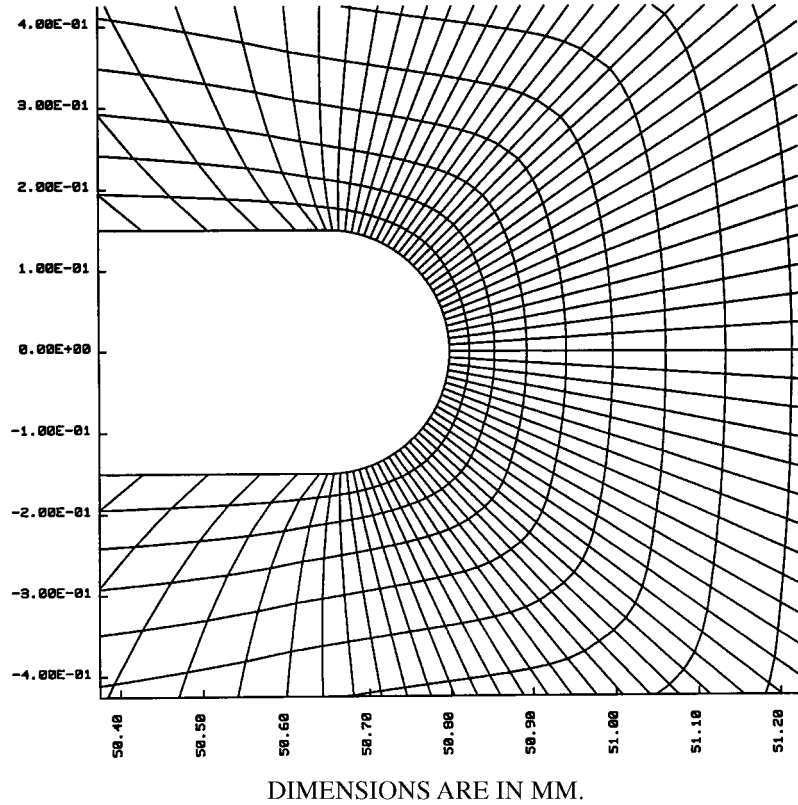
Figure 2. Details of the finite element mesh near the notch-tip.

initiates when the effective plastic strain at a point equals 0.5, we also delineate the effect of material and other parameters on the initiation of a failure mode.

2. Formulation of the problem

A schematic sketch of the problem studied is given in Figure 1. In the referential description equations governing the thermomechanical deformations of the projectile and the prenotched plate are

$$\rho J = \rho_0, \qquad J = \det \mathbf{F}, \tag{1}$$

$$\rho_0 \dot{\mathbf{V}} = \operatorname{Div} \mathbf{T}, \tag{2}$$

$$\mathbf{T}\mathbf{F}^T = \mathbf{F}\mathbf{T}^T, \tag{3}$$

$$\rho_0 \dot{e} = -\operatorname{Div} \mathbf{Q} + \operatorname{tr}(\mathbf{T}\dot{\mathbf{F}}^T). \tag{4}$$

Here ρ is the present mass density of a material particle whose mass density in the reference configuration is ρ_0, $\mathbf{F}$ the deformation gradient, $\mathbf{V}$ the velocity of a material particle, a super-imposed dot indicates the material time derivative, $\mathbf{T}$ the first Piola–Kirchhoff stress tensor, e the specific internal energy, $\mathbf{Q}$ the heat flux measured per unit reference area, and Div the divergence operator with respect to coordinates in the reference configuration. Here we assume
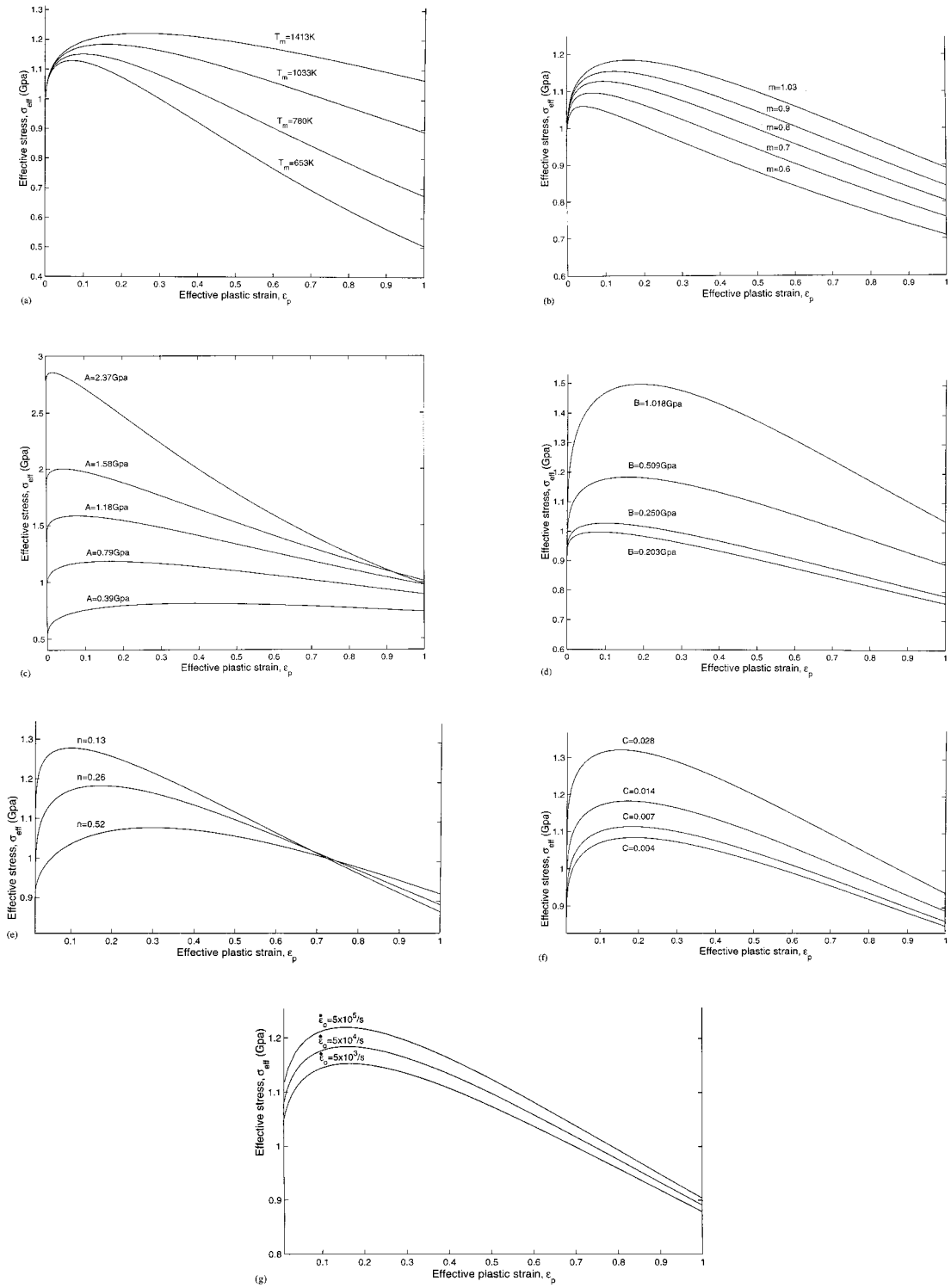
Figure 3(a–g). Effective stress vs. effective plastic strain during simple shearing deformations of a typical steel deformed at a nominal strain-rate of 50 000/s for different values of material parameters.

the deformations to be locally adiabatic, thus $\mathbf{Q} \equiv \mathbf{0}$. All of the plastic working is assumed to be converted into heating even though Farren and Taylor (1925) and Sulijoadikusumo and Dillon (1979) proposed that only 90 to 95 percent of plastic working is converted into heating. Mason et al. (1994b) have shown that the fraction of plastic working converted into heating depends upon the strain, strain-rate and the material of the body.

Both the projectile and the plate are assumed to be made of the same homogeneous and isotropic thermoviscoplastic material which is modeled by the following constitutive relations.

$$\boldsymbol{\sigma} = -p\mathbf{1} + \mathbf{s}, \qquad p = K(\rho/\rho_0 - 1), \qquad \boldsymbol{\sigma} = J^{-1}\mathbf{TF}^T, \tag{5}$$

$$\overset{\triangledown}{\boldsymbol{\sigma}} = \dot{\boldsymbol{\sigma}} + \mathbf{W}\boldsymbol{\sigma} - \boldsymbol{\sigma}\mathbf{W}, \qquad 2\mathbf{W} = \operatorname{grad} \mathbf{v} - (\operatorname{grad} \mathbf{v})^T, \tag{6}$$

$$\overset{\triangledown}{\mathbf{s}} = 2\mu\bar{\mathbf{D}}^e, \qquad \operatorname{tr} \mathbf{D}^p = 0, \qquad \bar{\mathbf{D}} = \mathbf{D} - \tfrac{1}{3} \operatorname{tr}(\mathbf{D})\mathbf{1}, \tag{7}$$

$$\dot{e} = c\dot{T} + \operatorname{tr}(\boldsymbol{\sigma}\mathbf{D}^e) - 3\alpha p\dot{T}, \quad 2\mathbf{D} = \operatorname{grad} \mathbf{v} + (\operatorname{grad} \mathbf{v})^T, \quad \mathbf{D}^e = \mathbf{D} - \mathbf{D}^p - \alpha\dot{T}\mathbf{1}, \tag{8}$$

$$\mathbf{D}^p = \Lambda\mathbf{s}, \qquad \sigma_{\text{eff}} = (\tfrac{3}{2} \operatorname{tr}(\mathbf{ss}^T))^{1/2}, \tag{9}$$

$$\sigma_m = (A + B(\varepsilon_p)^n)(1 + C \ln(\dot{\varepsilon}_p/\dot{\varepsilon}_0^p)) \left(1 - \left(\frac{T - T_0}{T_m - T_0}\right)^m\right), \tag{10}$$

$$\dot{\varepsilon}_p = (\tfrac{2}{3} \operatorname{tr}(\bar{\mathbf{D}}^p\bar{\mathbf{D}}^p))^{1/2}, \qquad \varepsilon_p = \int \dot{\varepsilon}_p \, dt, \tag{11}$$

$$\Lambda = 0 \text{ if either } \sigma_{\text{eff}} < \sigma_m \text{ or } \sigma_{\text{eff}} = \sigma_m \text{ and } \operatorname{tr}(\mathbf{s}\overset{\triangledown}{\mathbf{s}}) \leqslant 0, \tag{12}$$

and

$$\Lambda > 0 \text{ if either } \sigma_{\text{eff}} > \sigma_m \text{ or } \sigma_{\text{eff}} = \sigma_m \text{ and } \operatorname{tr}(\mathbf{s}\overset{\triangledown}{\mathbf{s}}) > 0. \tag{13}$$

Whenever (13) holds Λ is a solution of the nonlinear equation

$$\sigma_{\text{eff}} = \sigma_m. \tag{14}$$

Here $\boldsymbol{\sigma}$ is the Cauchy stress tensor, σ_{eff} the equivalent or the effective stress, $\mathbf{s}$ the deviatoric Cauchy stress tensor, p the pressure, K the bulk modulus, α the coefficient of thermal expansion, $\overset{\triangledown}{\boldsymbol{\sigma}}$ the Jaumann derivative of $\boldsymbol{\sigma}$, $\mathbf{W}$ the spin tensor, μ the shear modulus, $\mathbf{D}$ the strain-rate tensor, $\bar{\mathbf{D}}$ the deviatoric strain-rate tensor, T the present temperature of a material particle, and grad the gradient operator with respect to coordinates in the present configuration. The strain-rate tensor is assumed to have an additive decomposition into an elastic part, $\mathbf{D}^e$, a plastic part, $\mathbf{D}^p$, and the strain-rate $\alpha\dot{T}\mathbf{1}$ due to thermal expansion. Equation $(9)_1$ states that $\mathbf{D}^p$ is parallel to $\mathbf{s}$, and (14) is the von-Mises yield criterion with the present value of the yield stress depending on the effective plastic strain, ε_p, the effective plastic strain-rate, $\dot{\varepsilon}_p$, and the nondimensional temperature, $(T - T_0)/(T_m - T_0)$; here T_0 is the reference temperature and T_m is related to the melting temperature of the material. Equation (10) is the Johnson–Cook relation expressing the effective stress σ_m in terms of ε_p, $\dot{\varepsilon}_p$ and T. In (10) A is the yield stress of the material in a quasistatic simple tension or compression test, parameters B
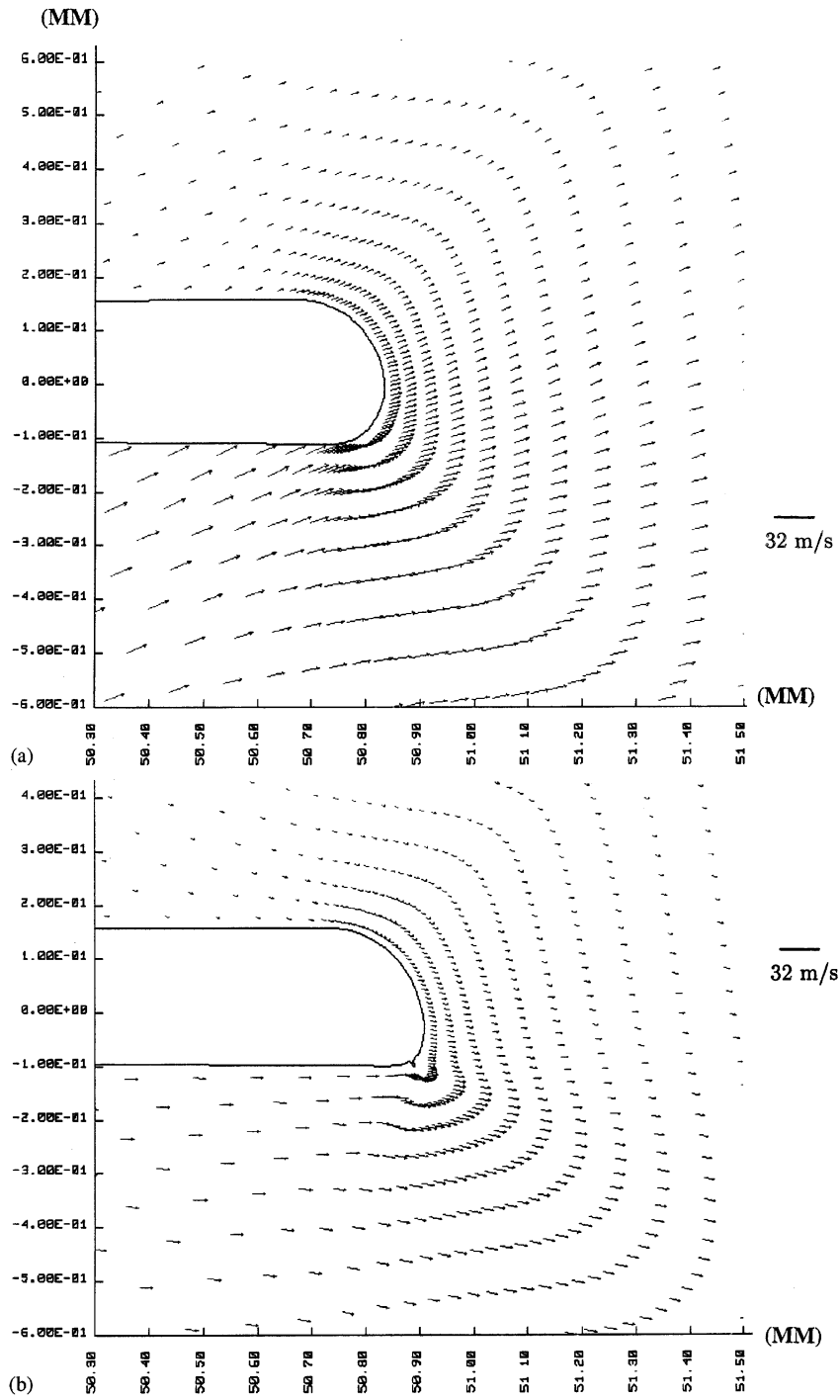
Figure 4. Velocity field, at (a) $t = 13\ \mu$s, and (b) $t = 23.5\ \mu$s, in the region surrounding the notch-tip ($m = 0.6$).
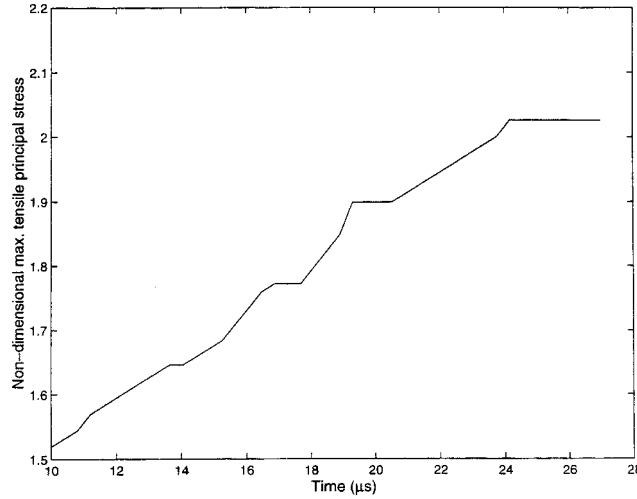
Figure 5. Time-history of the nondimensional maximum tensile principal stress, (σ/σ_0), in the vicinity of the point on the notch surface that makes, in the reference configuration, an angle of $70°$ with the notch-axis ($m = 0.6$).

and n characterize the strain hardening of the material, C and $\dot{\varepsilon}_0^p$ the strain-rate hardening of the material, and T_m and m the thermal softening of the material. Johnson and Cook (1983) proposed the empirical relation (10) based on torsional test data at different strain-rates and temperatures. Batra and Kim (1990) calibrated the Johnson–Cook relation, the power law, the Litonski relation, the Wright–Batra relation and the Bodner–Partom law against the test data of Marchand and Duffy (1988) and used them to study the pre- and post-localization response of the material deformed in simple shear. A defect was modeled by a nonuniform distribution of the initial temperature. They found that deformations of the material until the initiation of a shear band were essentially the same for each one of the constitutive relations; however, the postlocalization response with each constitutive relation was significantly different. This work and a similar study by Batra and Jayachandran (1992) on steady state penetration of a thermoviscoplastic target by a rigid cylindrical rod suggest that the choice of the constitutive relation is less critical for studying the deformations of a body until the deformation localizes.

Initially the prenotched plate is at rest, stress free and at a uniform temperature T_0. The projectile is stress free, at a uniform temperature T_0, is moving with a uniform velocity $\mathbf{V}_0$ parallel to the axis of the notch, and at time $t = 0$ impacts the prenotched plate at normal incidence.

All bounding surfaces of the projectile and the prenotched plate are thermally insulated, and all of these except for the impacted faces are traction free. At the contact surface

$$[\mathbf{V} \cdot \mathbf{n}] = 0, \qquad [\mathbf{n} \cdot \boldsymbol{\sigma}\mathbf{n}] = 0, \qquad \mathbf{f}_t = -(\mathbf{n} \cdot \boldsymbol{\sigma}\mathbf{n})(\mu_s + (\mu_k - \mu_s)\,e^{-\beta v_{\mathrm{rel}}})\mathbf{t},$$

$$\mathbf{t} = \mathbf{v}_{\mathrm{rel}}/|\mathbf{v}_{\mathrm{rel}}|, \tag{15}$$

where $[f]$ denotes the jump in the values of f on the two sides of the contact surface, $\mathbf{n}$ is a unit outward normal to the surface, $\mathbf{f}_t$ is the tangential traction acting along the unit tangent vector $\mathbf{t}$, and $\mathbf{v}_{\mathrm{rel}}$ equals the relative velocity of sliding between the two contacting points. μ_s and μ_k are the static and the kinetic coefficients of friction, respectively, and β describes the dependence of the frictional force upon the relative speed of sliding. Values of μ_s, μ_k and β depend upon the roughness of the contacting surfaces.

(a)

(b)
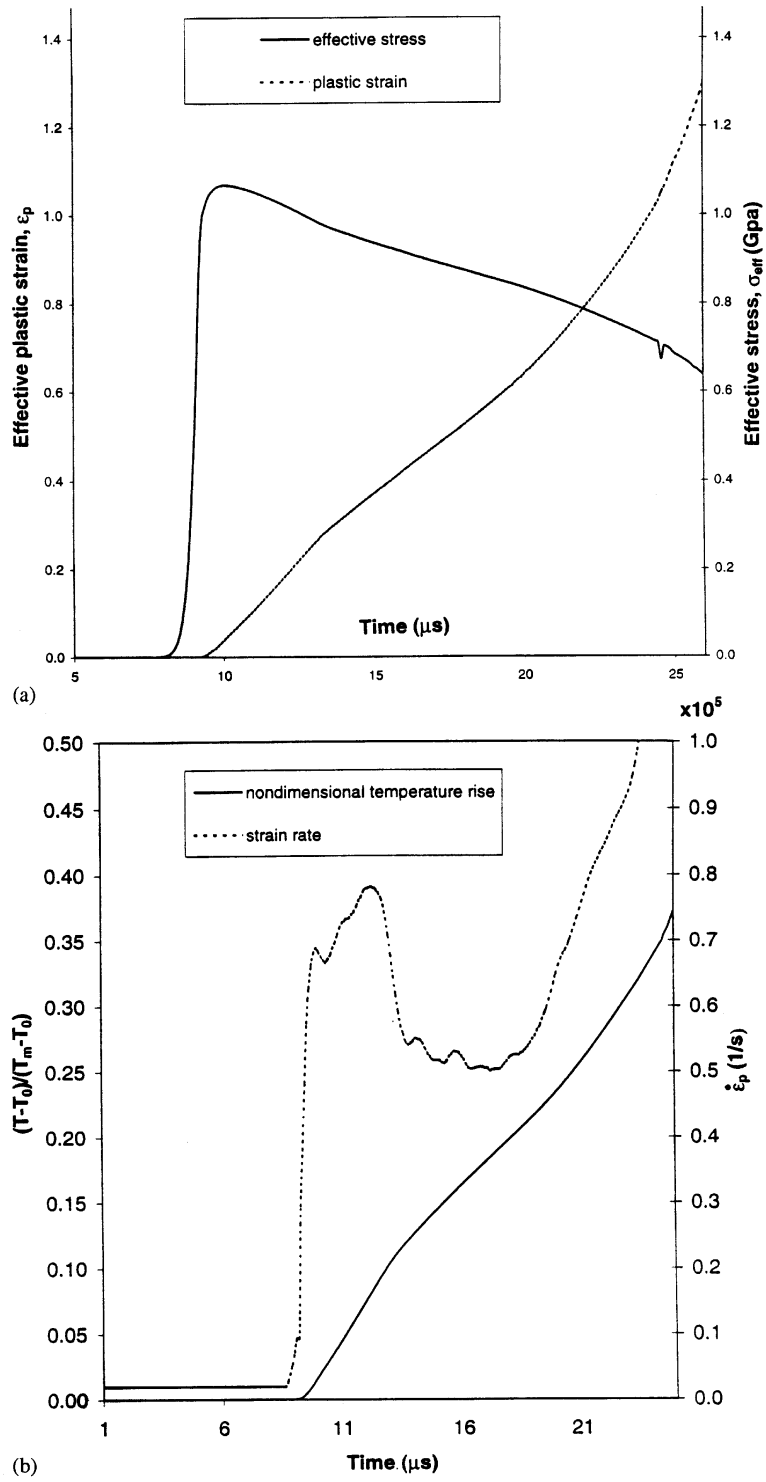
Figure 6(a–b). Time histories of the effective plastic strain, the effective plastic strain-rate, the effective stress and the temperature rise at a point on the notch surface that makes an angle of $-45°$ with the notch-axis in the reference configuration.

(a)   ALL DIMENSIONS ARE IN MM.

ELEMENT E

(b)   ALL DIMENSIONS ARE IN MM.
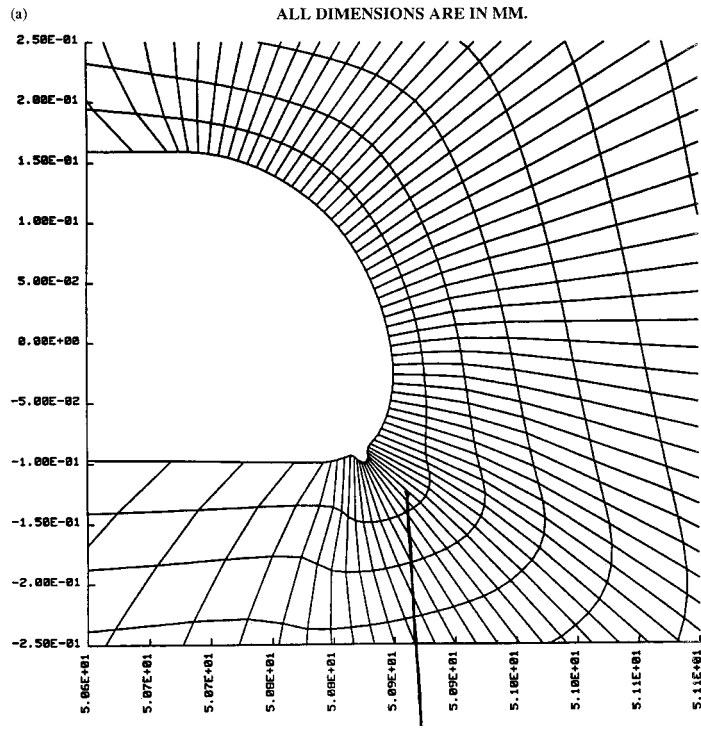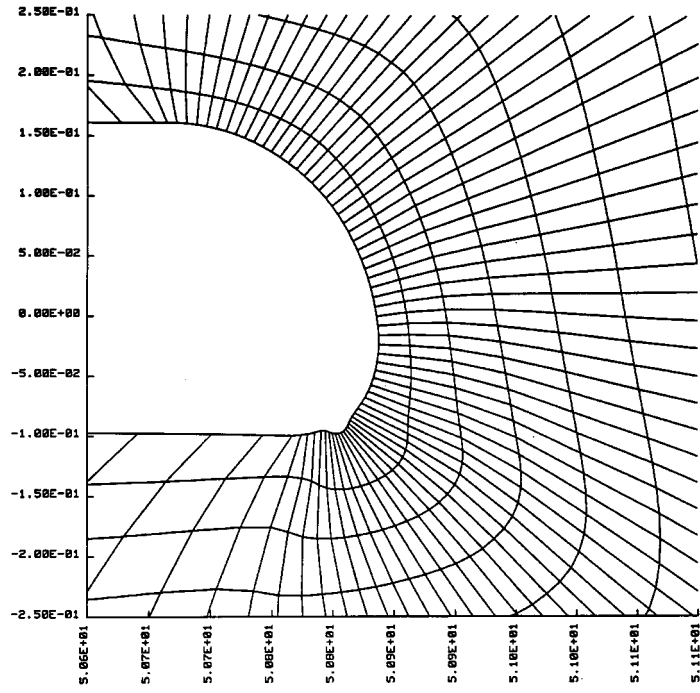
Figure 7a,b.

(c)   ALL DIMENSIONS ARE IN MM.

(d)   ALL DIMENSIONS ARE IN MM.
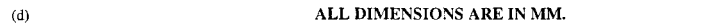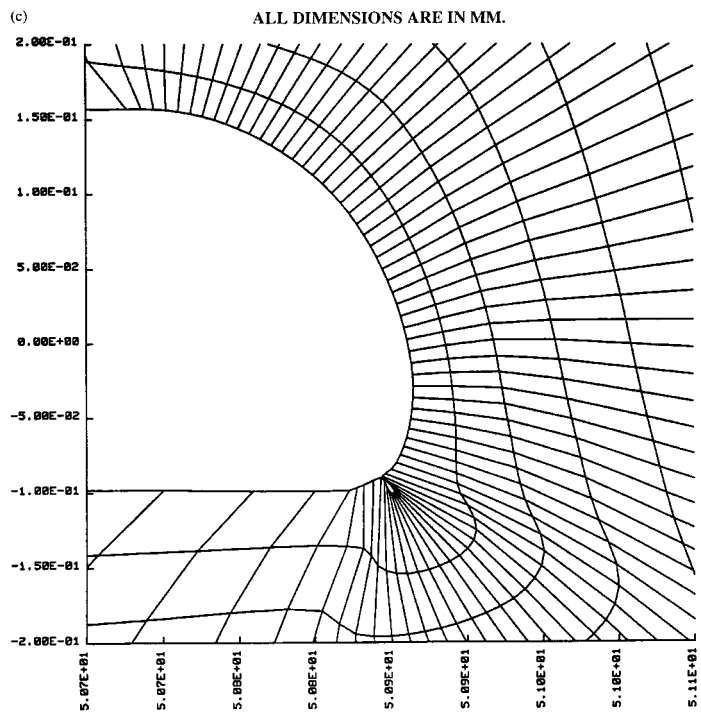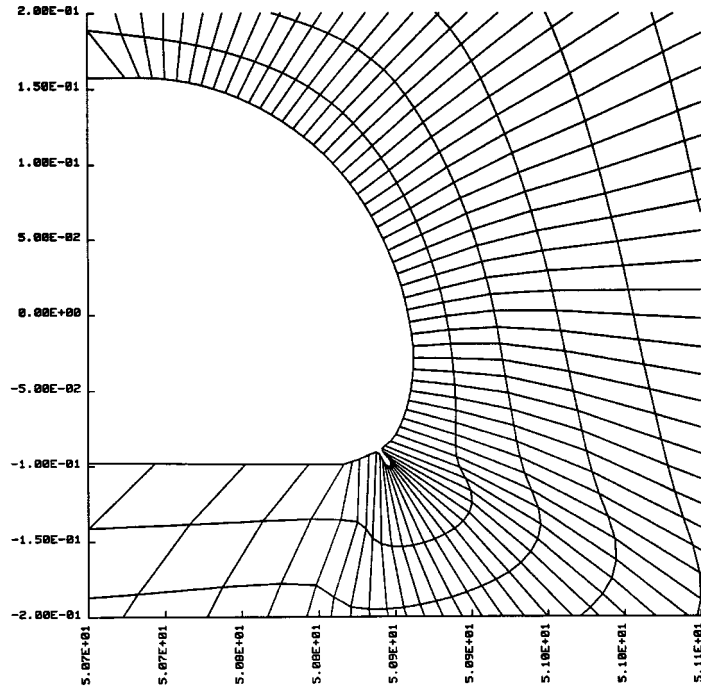
Figure 7. Deformed shape of the material with $m = 0.6$ near the notch-tip at $t = 20$, 22, 24 and 24.5 μs.
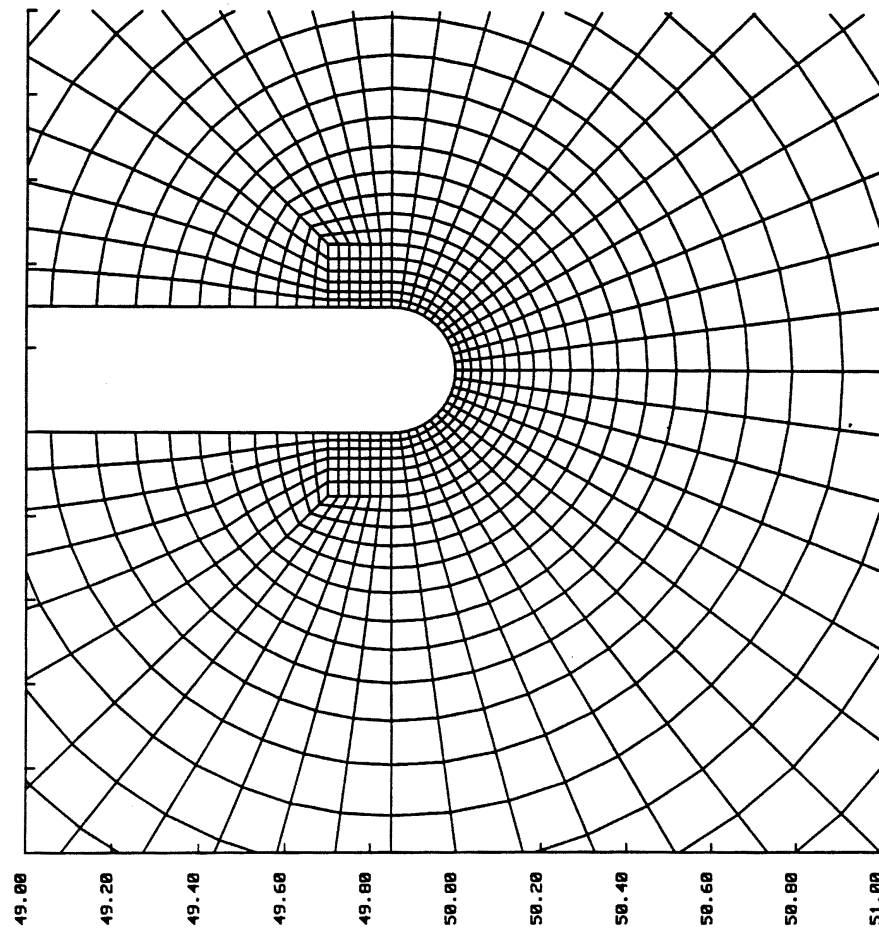
ALL DIMENSIONS ARE IN MM.

Figure 8. Details of an alternate finite element mesh near the notch-tip.

In order to determine whether a brittle or a ductile failure initiates first, the brittle failure is assumed to occur at a point when the maximum tensile principal stress there equals twice the quasistatic yield stress of the material in a simple tension or compression test. The criterion for the initiation of a shear band is described in Section 3. However, no such failure or fracture criterion has been implemented in the code; thus a material point can undergo unlimited plastic deformations. Even though the projectile is assumed to be deformable, details of its deformations are not described in order to stay focussed on the deformations of the plate material near the notch-tip.

3. Computation and discussion of results

We employ the large scale explicit finite element code DYNA2D developed by Whirley et al. (1992) to analyze the aforestated problem. It uses four noded quadrilateral elements with one-
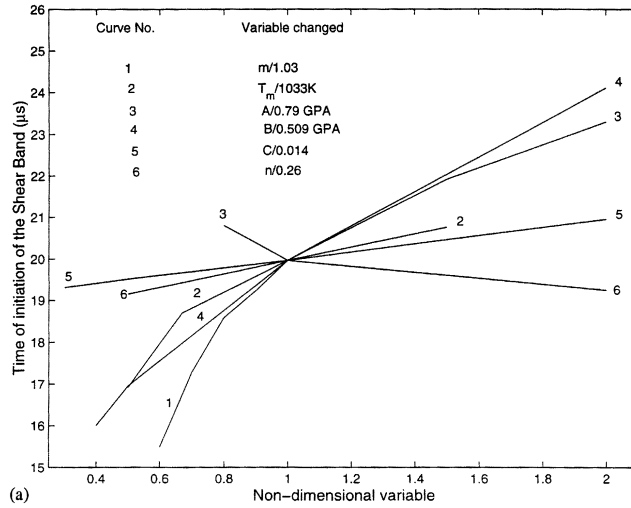
Figure 9a. Effect of different material variables on the time of initiation of a shear band. A shear band is assumed to initiate when the maximum effective plastic strain at any point equals 0.5.
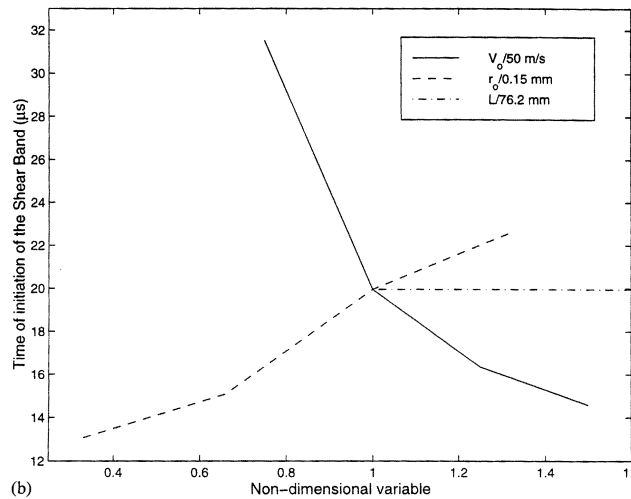
Figure 9b. Effect of impact speed, notch-tip radius and the length of the projectile on the time of initiation of a shear band.

point integration rule, the conditionally stable central-difference method for time integration, and an hour-glass control algorithm to suppress the spurious modes. The finite element mesh shown in Figure 2 has sixty elements around the notch-tip, and the element size gradually increases with distance from the notch-tip. For one set of material parameters results were also computed with two other meshes with 30 and 48 elements around the notch-tip; otherwise the mesh design was similar to that shown in Figure 2. The three meshes gave essentially identical results. Results presented herein are obtained with the mesh depicted in Figure 2 with 7.85 μm $\times 23.6$ μm elements abutting the notch-tip of radius 0.15 mm; the size of an element near the notch-tip is proportional to the radius of the notch-tip. The hour-glass viscosity coefficient was set equal to 0.4 in order to suppress spurious modes. Results for one case were also computed with the hour-glass viscosity equal to 0.1 and were found to be virtually indistinguishable
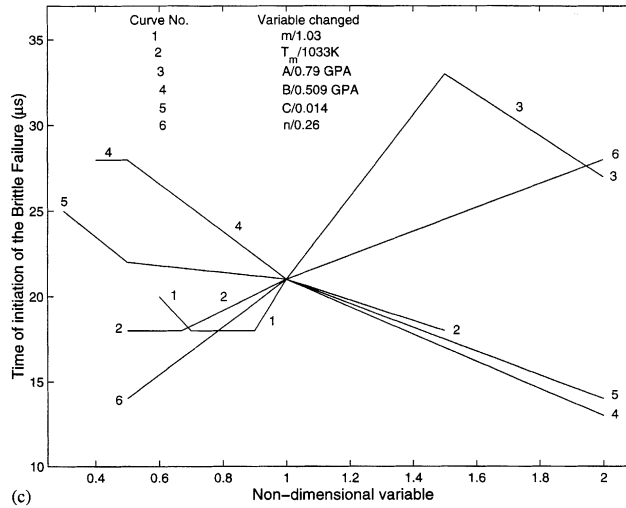
Figure 9c. Effect of different material parameters on the time of initiation of brittle failure. The brittle failure is assumed to occur when the maximum tensile principal stress at a point equals twice the yield stress of the material in a quasistatic simple tension/compression test.
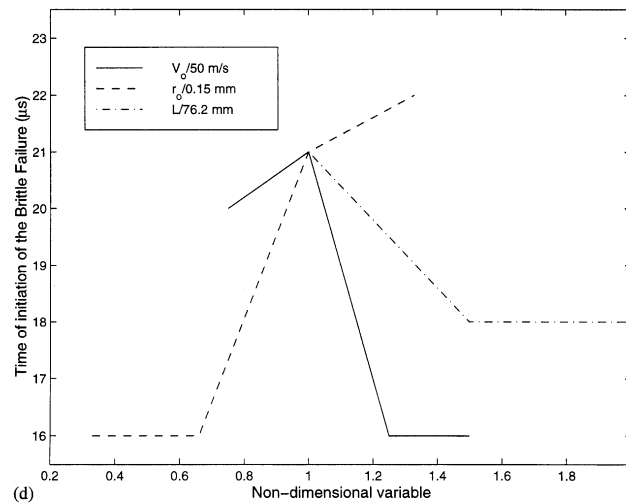
Figure 9d. Effect of impact speed, notch-tip radius and the length of the projectile on the time of initiation of brittle failure.

from those for hour-glass viscosity equal to 0.4. Because of the assumption of locally adiabatic deformations, the energy equation is trivially integrated, and the size of the time step is governed by the mechanical problem. The time step size equals 0.6 times the time taken by the dilatational wave to travel the shortest dimension of any element in the mesh. The time step size is greatly reduced as the elements get distorted during the deformation process.

In DYNA2D the effects of thermal expansion are neglected. This has no effect on the computed plastic strains since the plastic strain-rate is proportional to the deviatoric Cauchy stress tensor. Material points where the maximum tensile principal stress occurs are not heated much because of the small plastic strains induced there. Thus the computed values of the maximum tensile principal stress should be reasonable.

(a)
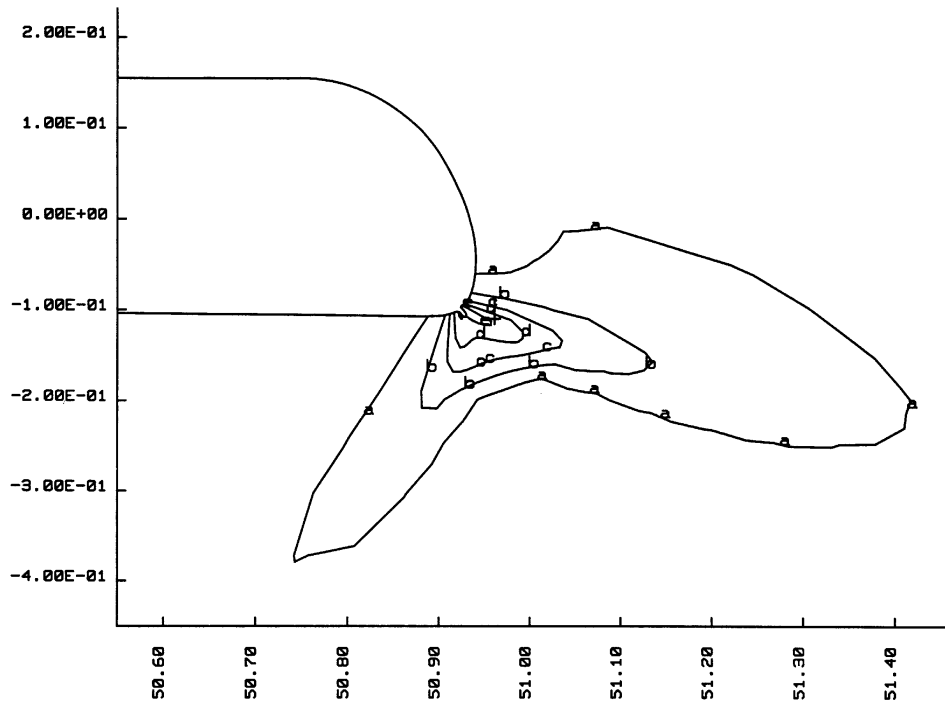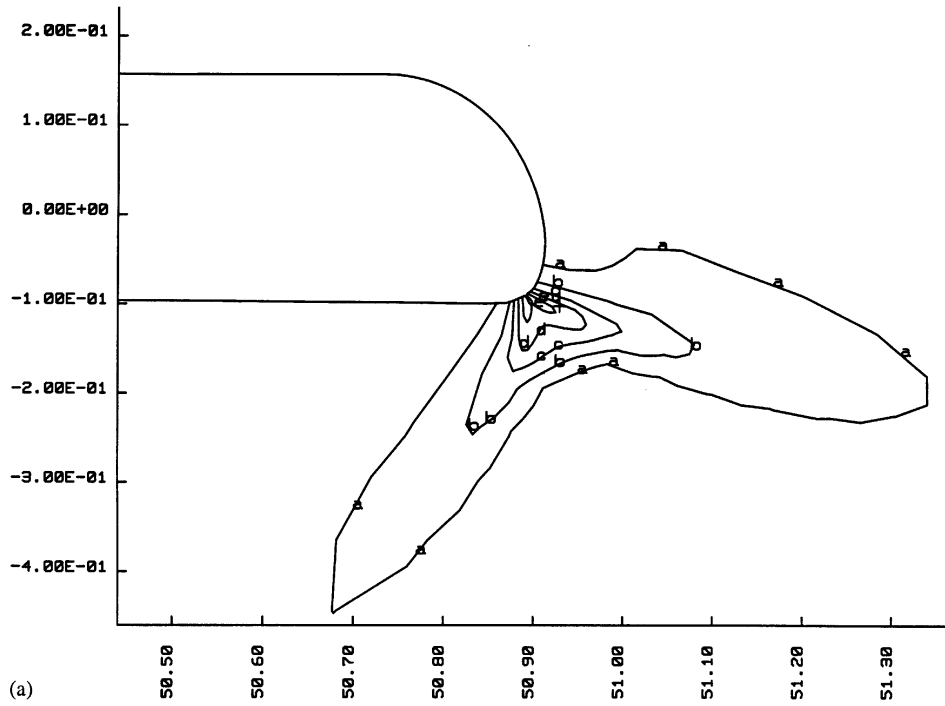
(b)   **DIMENSIONS ARE IN MM.**

Figure 10a,b.

(c)

(d)

DIMENSIONS ARE IN MM.

Figure 10c,d.

(MM)

```
6.00E-01 ⌐

5.00E-01 ⌐

4.00E-01 ⌐            a= .17E+00
                      b= .34E+00
3.00E-01 ⌐            c= .51E+00
                      d= .67E+00
2.00E-01 ⌐            e= .84E+00
```
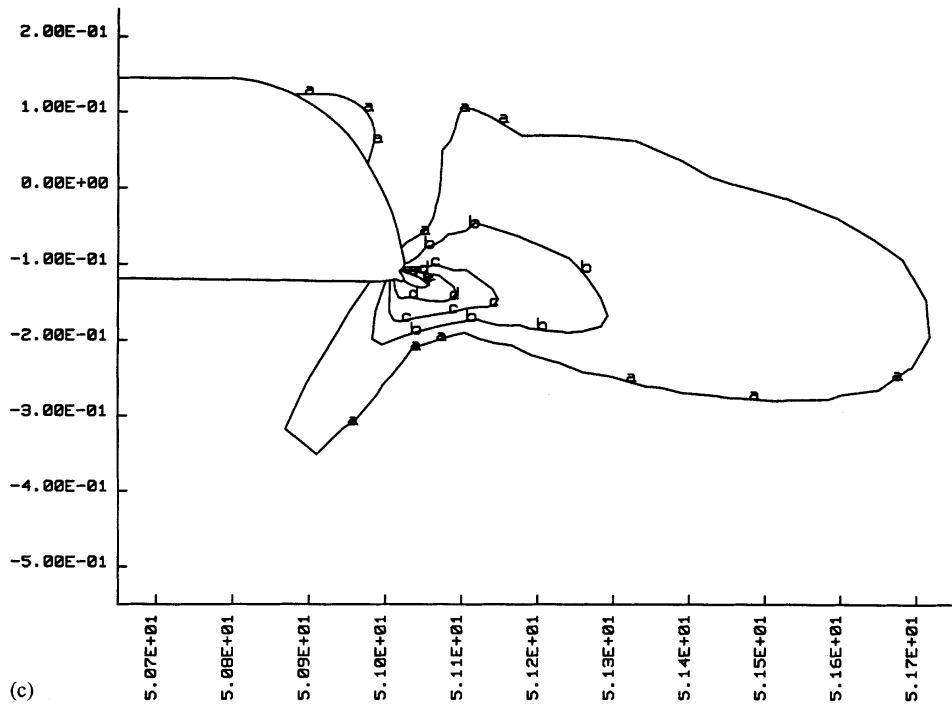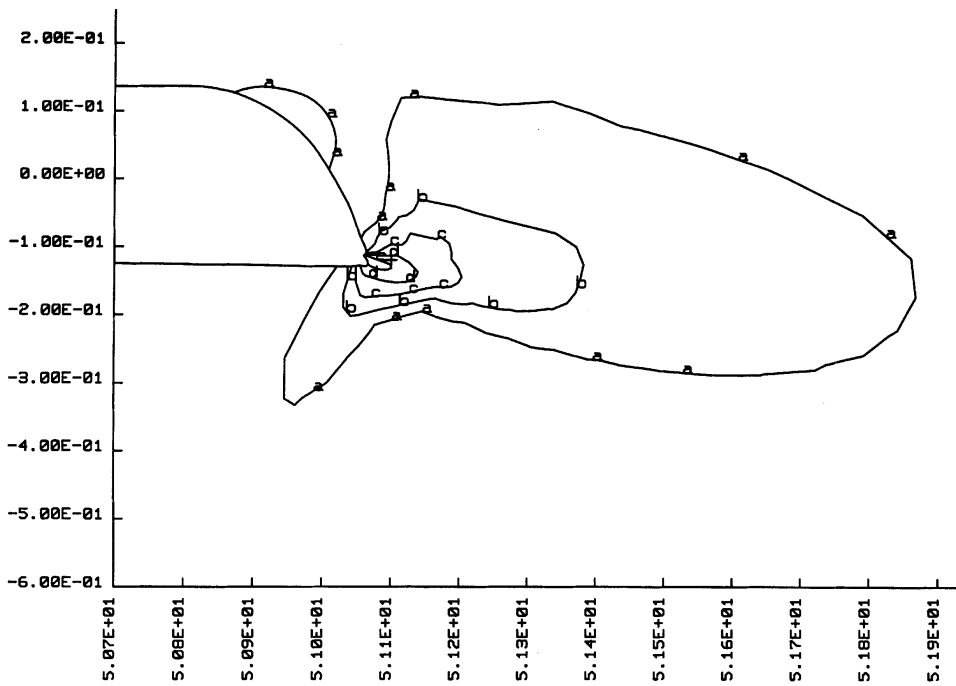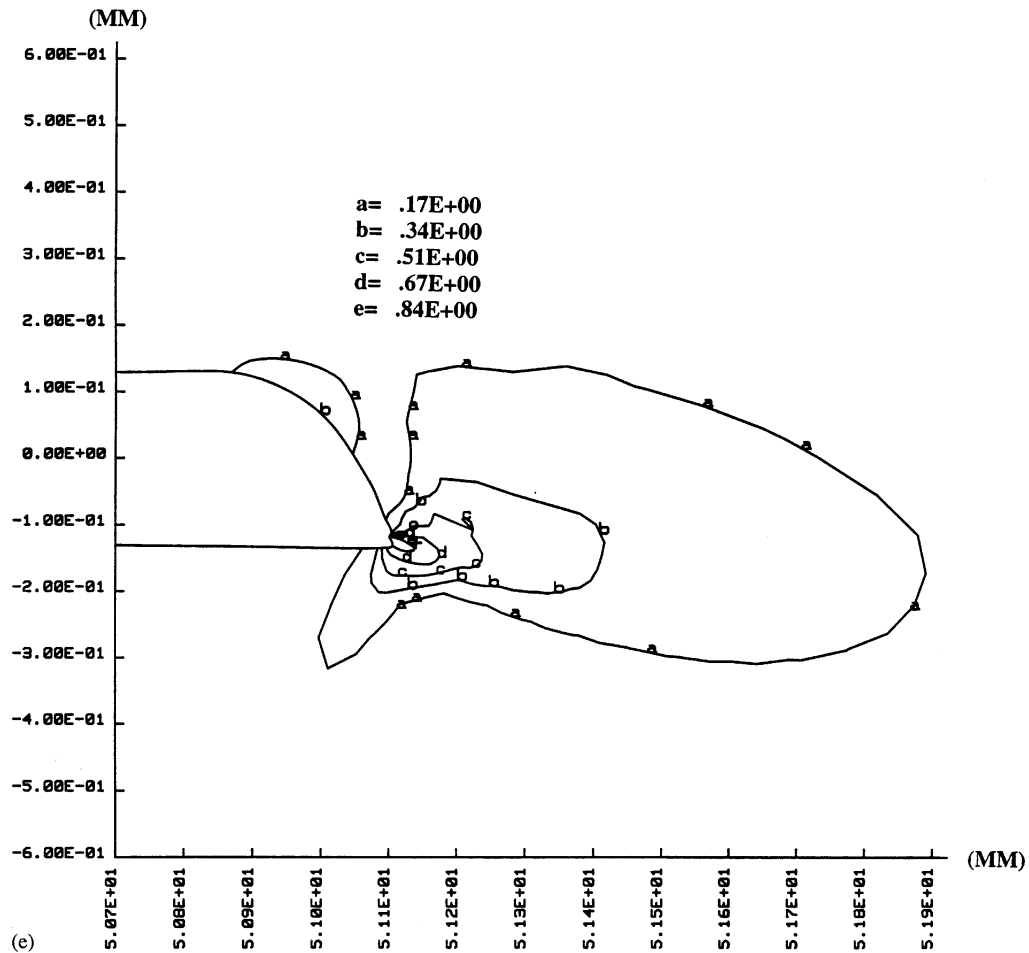

Figure 10. Contours of the effective plastic strain for different values of m when the maximum effective plastic strain at any point near the notch-tip equals 1.0; (a) $m = 0.6$, (b) $m = 0.7$, (c) $m = 0.8$, (d) $m = 0.9$, (e) $m = 1.03$. The corresponding times are 24.25, 27, 31, 33 and 35 μs respectively. Values of ε_p for different contours are indicated in Figure 10(e).

We analyze the effect on the deformations near the notch-tip of each material parameter in the Johnson–Cook relation, the notch-tip radius, impact speed and the length of the projectile which controls the duration of the loading pulse. When conducting the parametric studies, only one variable is changed at a time. Base values of the material (for a typical steel) and geometric parameters used to compute numerical results are listed below.

$$A = 791.2\,\text{MPa}, \qquad B = 509.51\,\text{MPa}, \qquad C = 0.014, \qquad n = 0.26, \qquad \dot{\varepsilon}_0^p = 1/\text{s},$$

$$m = 1.03, \qquad K = 157\,\text{GPa}, \qquad \mu = 76\,\text{GPa}, \qquad T_m = 1033\,\text{K},$$

$$c = 452\,\text{J}/(\text{kg K}), \qquad \rho_0 = 7850\,\text{kg/m}^3, \qquad r_0 = 0.15\,\text{mm}, \qquad V_0 = 50\,\text{m/s},$$

$$\mu_s = 0.18, \qquad \mu_k = 0.05 \text{ and } \beta = 0.0055.$$

(16)

The values of material parameters in the Johnson–Cook relation are taken from Rajendran's report (1992). For large variations in temperature, as are likely to occur near the notch-tip,

(a)

(b)
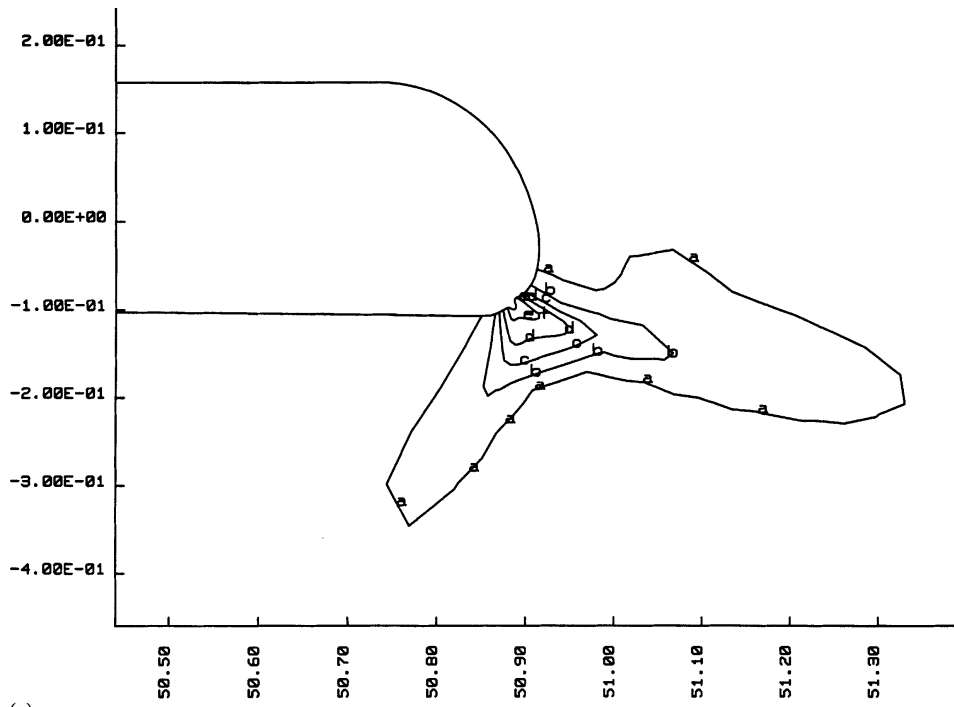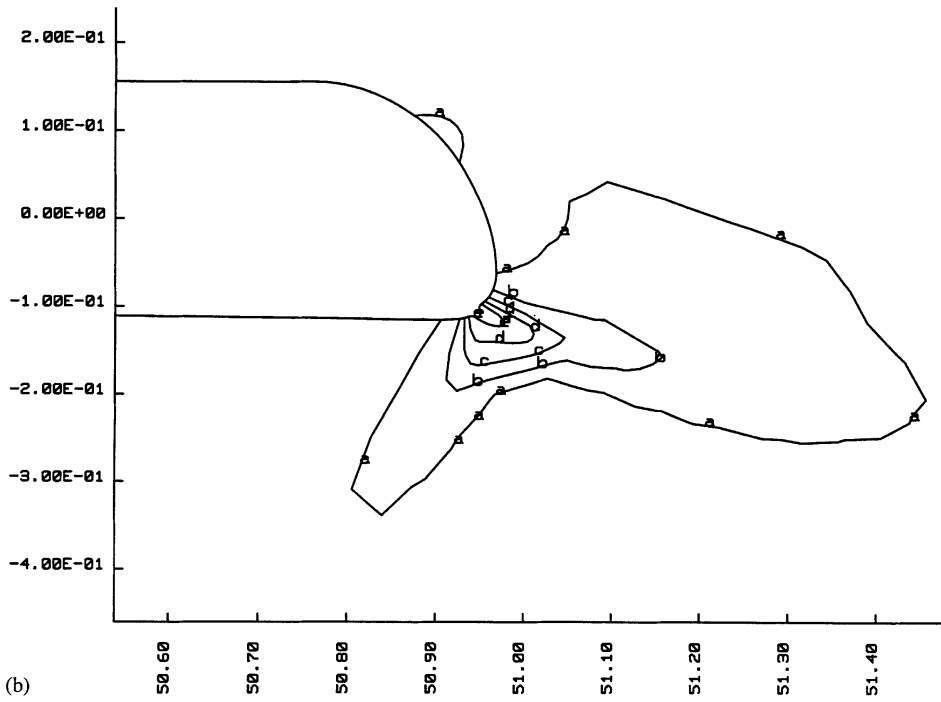
DIMENSIONS ARE IN MM.

Figure 11a,b.
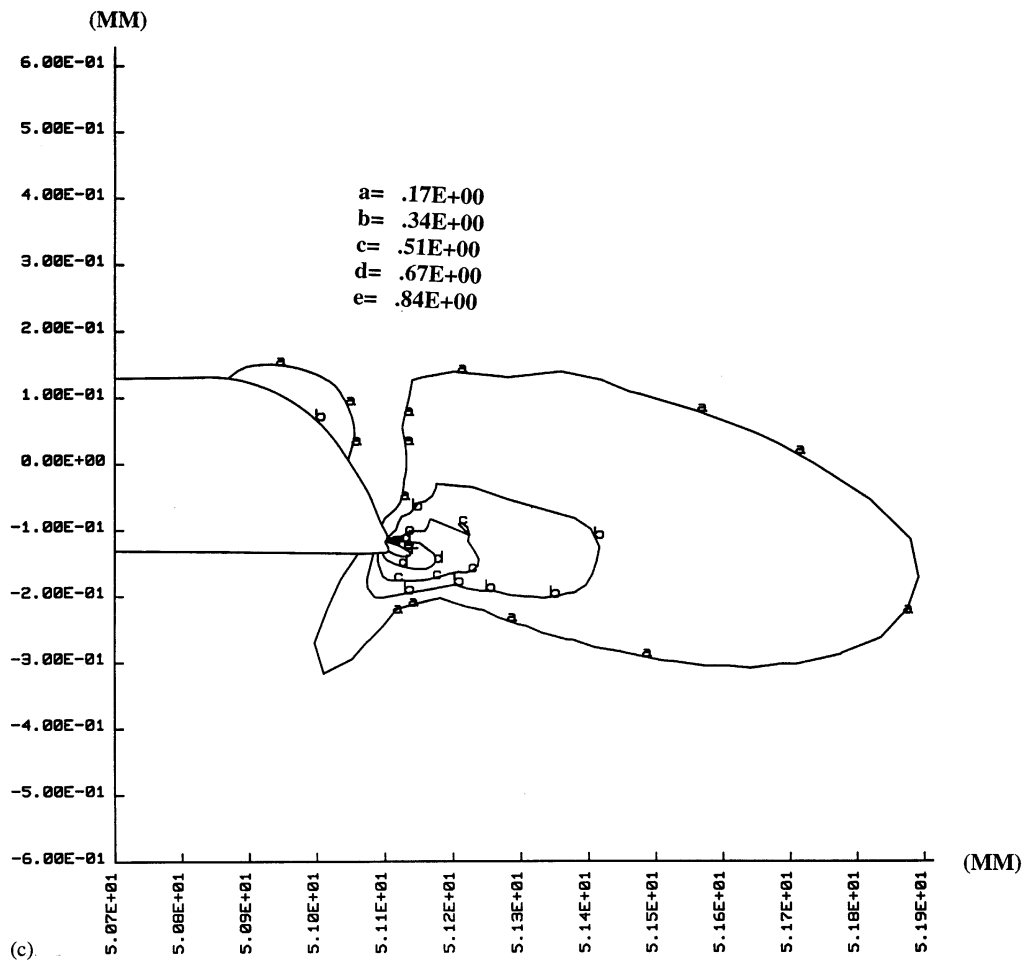
Figure 11. Contours of the effective plastic strain for different values of T_m when the maximum effective plastic strain at any point near the notch-tip equals 1.0; (a) $T_m = 653$ K, (b) $T_m = 780$ K, (c) $T_m = 1033$ K. The corresponding times are 24, 28 and 35 μs respectively. Values of ε_p for different contours are indicated in Figure 11(c).

nearly all of these material parameters depend upon the temperature, e.g. see Klepaczo et al. (1987). However, this temperature dependence has not been considered here mainly because of the lack of such data.

By assuming that the plate material is linear elastic, a plane strain state of deformation prevails, velocity is instantaneously applied normal to the impact face, and Poisson's ratio for the material of the plate equals 0.25, Lee and Freund (1990) found that the near-field mode-mixity parameter equals -0.25 over the time interval of interest, i.e., before waves reflected from the far end have arrived at the notch tip. Thus both mode-I and mode-II deformations occur near the notch-tip but the latter are predominant. In an attempt to delineate which parameters might strongly influence deformations near the notch-tip of a thermoviscoplastic plate, we have used DYNA2D to numerically simulate simple shearing deformations of a homogeneous block of the material at an average strain-rate of 5×10^4/s. It is close to the maximum value of the effective plastic strain-rate computed in the simulations of the Kalthoff

(a)

(b)

DIMENSIONS ARE IN MM.

Figure 12a,b.

(c)
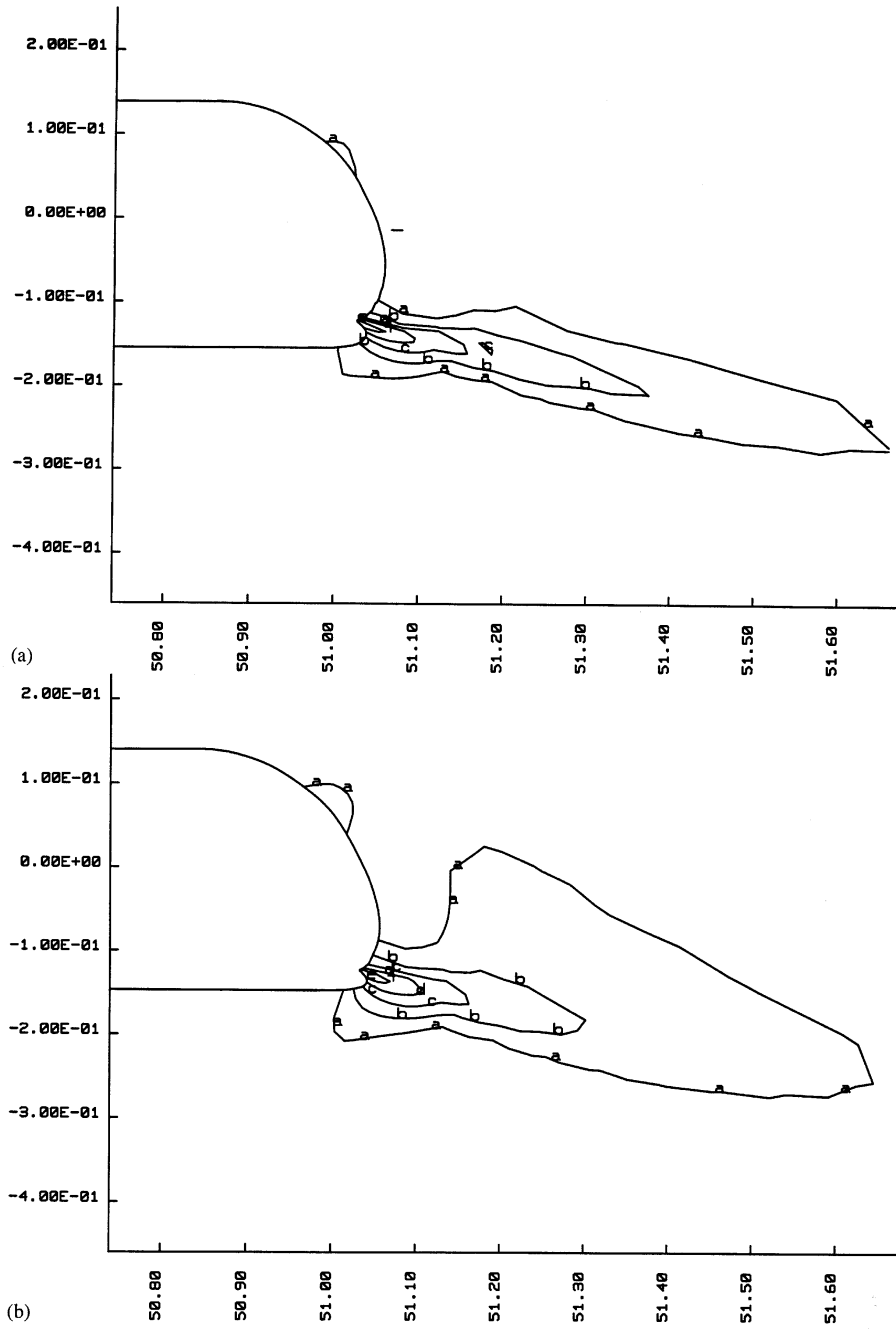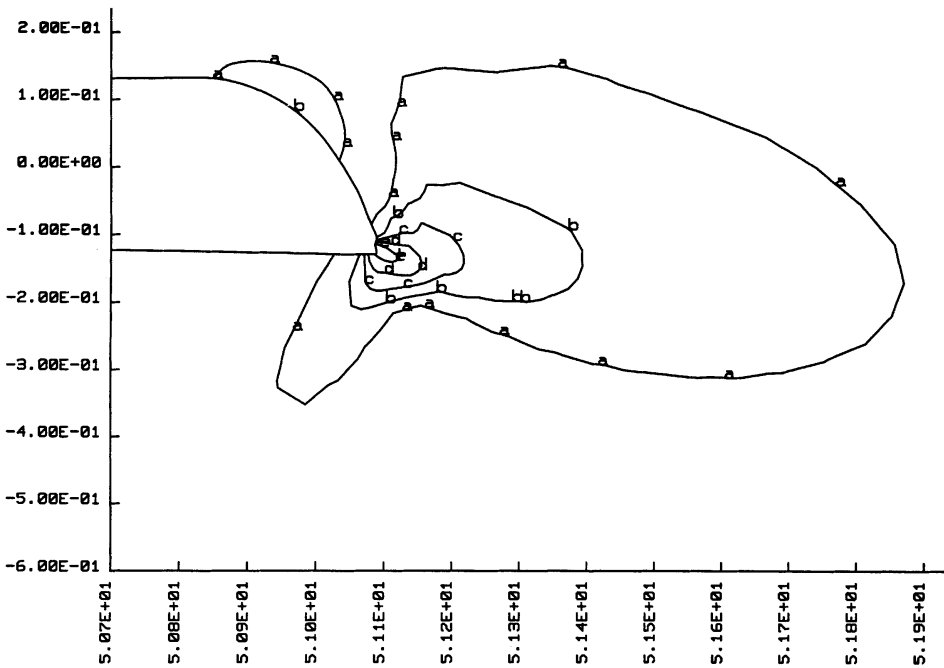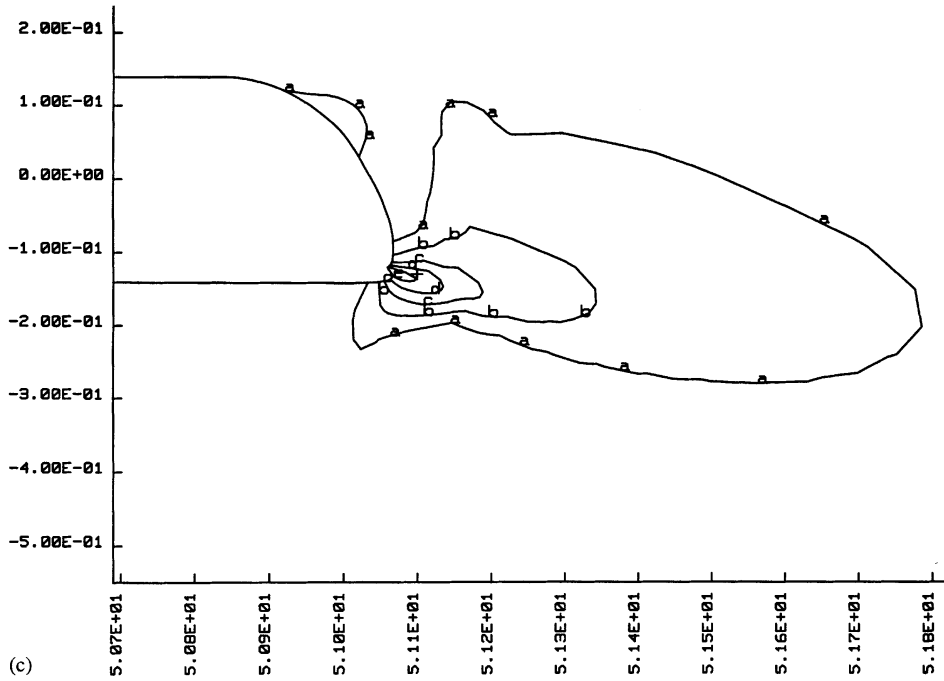
(d)   **DIMENSIONS ARE IN MM.**

Figure 12. Contours of the effective plastic strain for different values of A when the maximum effective plastic strain at any point near the notch-tip equals 1.0; (a) $A = 2.376$ GPa, (b) $A = 1.584$ GPa, (c) $A = 1.18$ GPa, (d) $A = 0.63$ GPa. The corresponding times are 30.75, 31, 32 and 36 μs respectively. Values of ε_p for different contours are: $a = 0.17$, $b = 0.34$, $c = 0.50$, $d = 0.67$, $e = 0.84$.
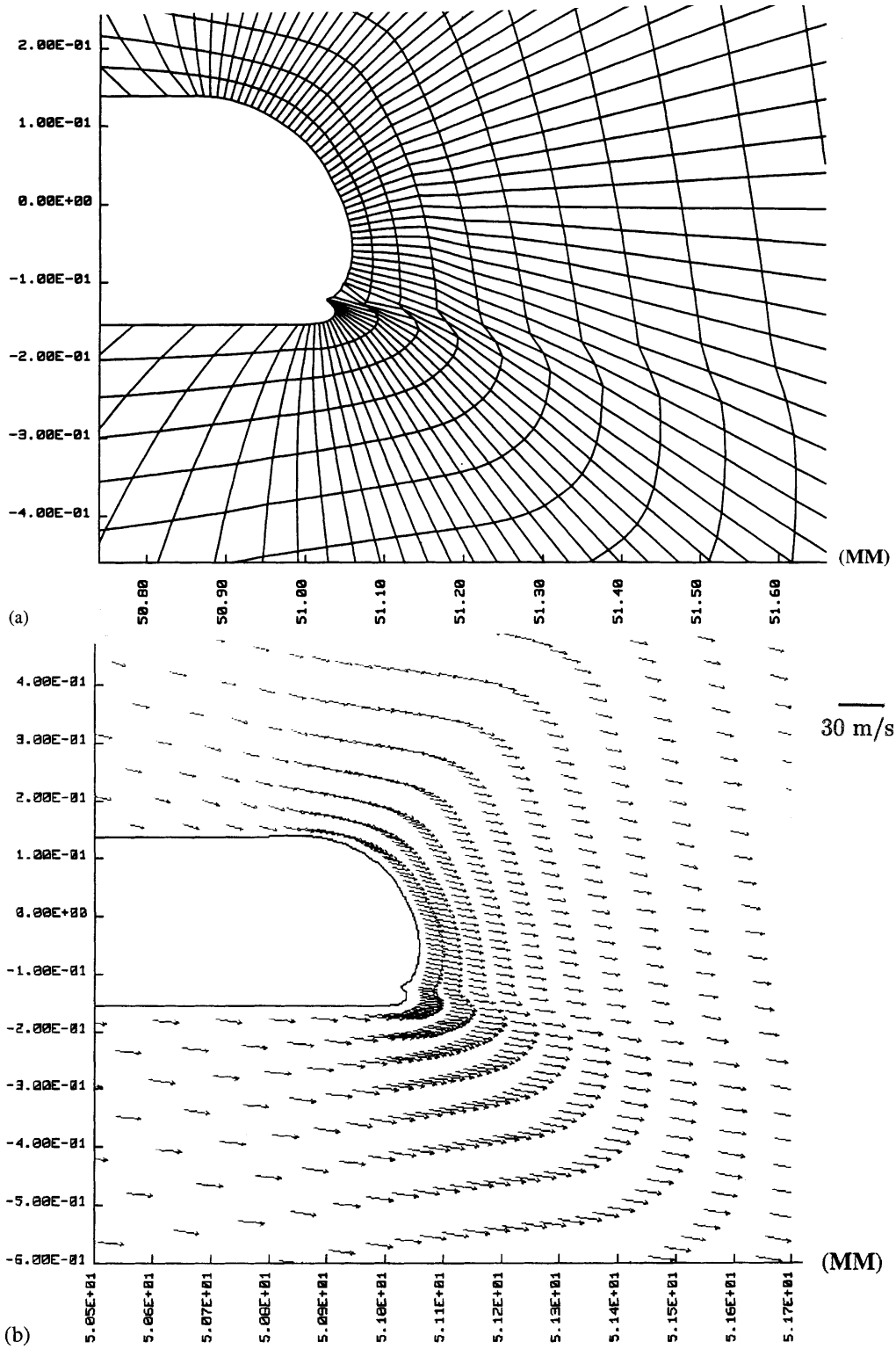
Figure 13. For $A = 2.376\,\text{GPa}$, (a) the deformed mesh and (b) the velocity field near the notch surface at $t = 37.5\,\mu\text{s}$.

a= .13E+00
b= .25E+00
c= .38E+00
d= .51E+00
e= .63E+00
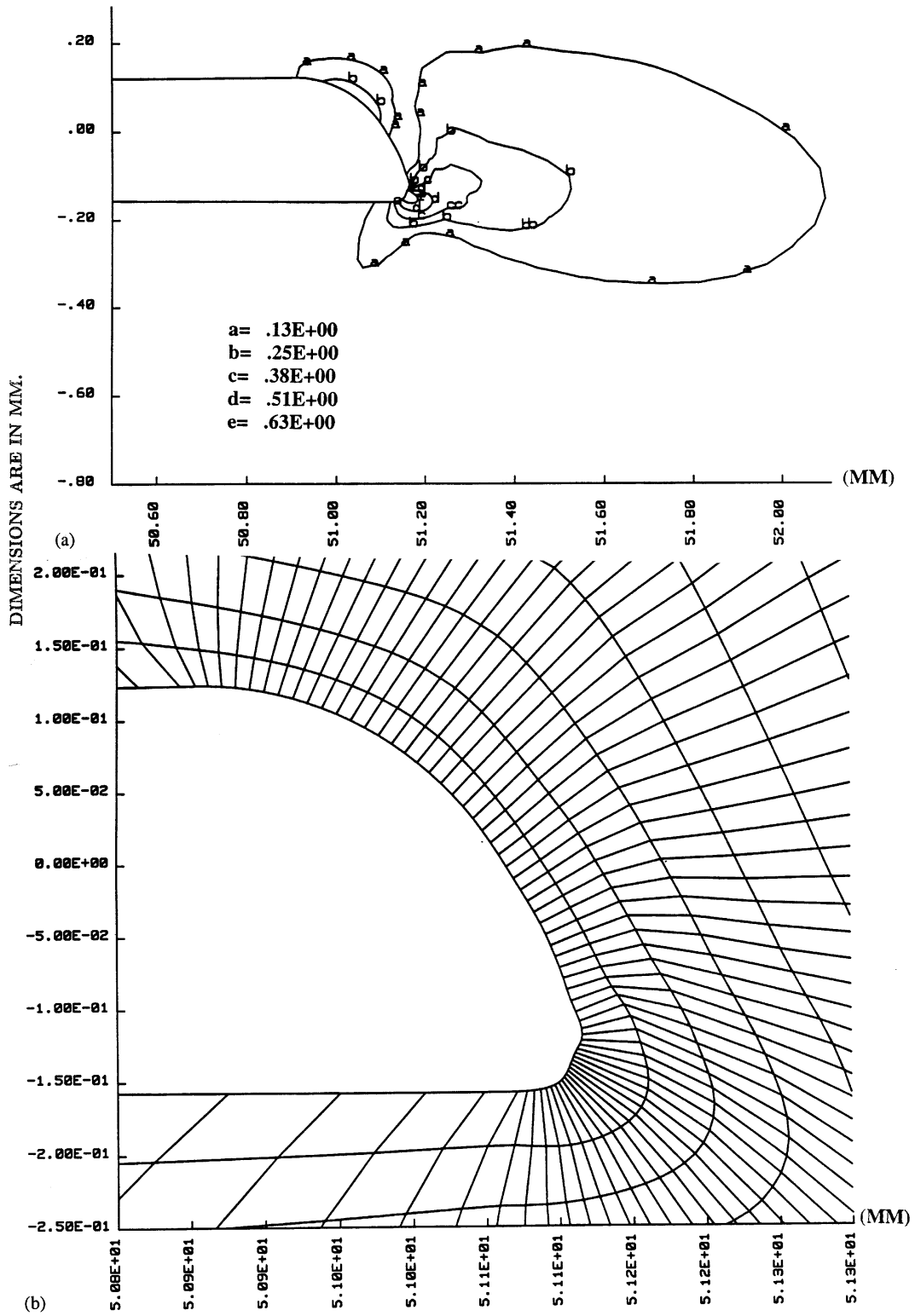
Figure 14. Contours of the effective plastic strain and the deformed notch-tip at $t = 38\,\mu$s for a material with $B = 1.018\,$GPa.
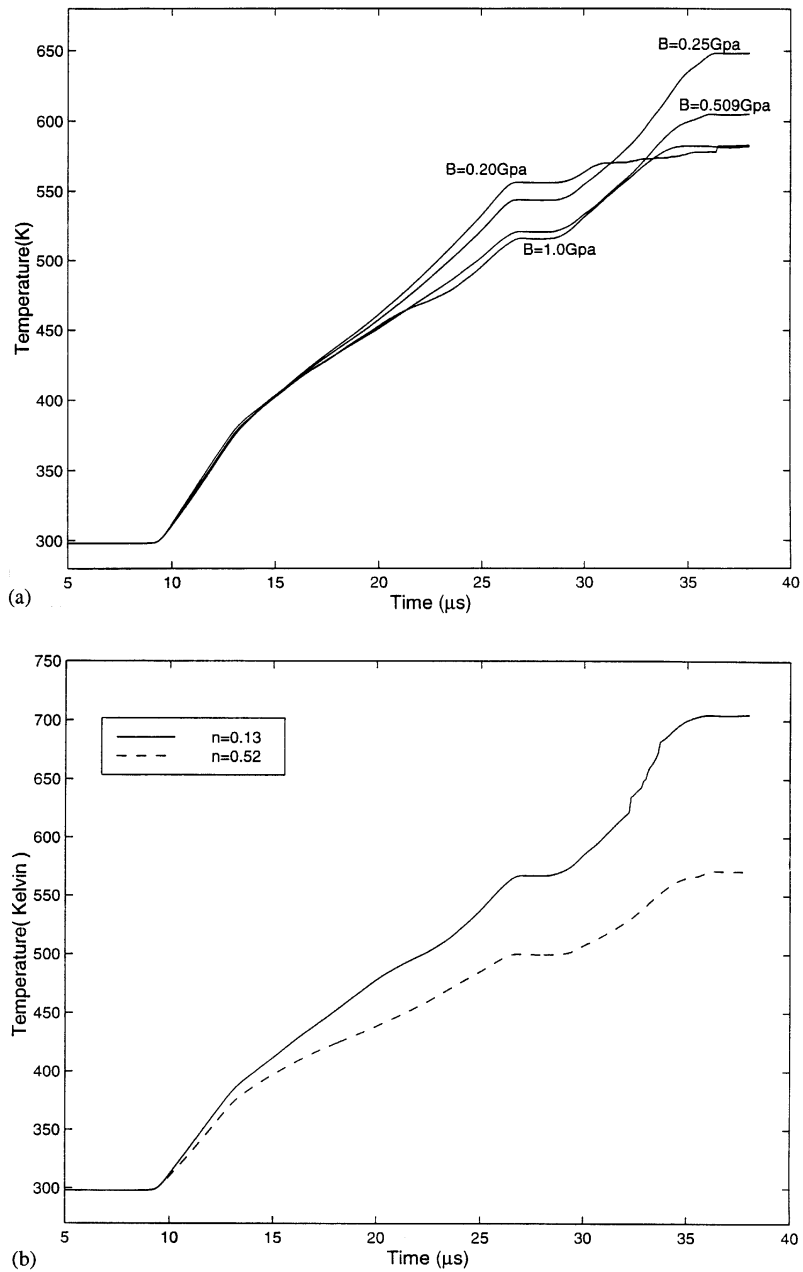
Figure 15. Time histories of the temperature in element E (see Figure 7(b) for its location) for (a) four values of B and (b) two values of n.

experiment. Figures 3(a) through 3(g) depict the effective stress vs. the effective plastic strain curves for different values of material parameters A, B, C, n, m, T_m, and the nominal shear strain-rate $\dot{\varepsilon}_0$. It is clear that lower values of T_m and higher values of A increase the magnitude of the initial negative slope of the effective stress vs. the effective plastic strain curves. For a simple shearing problem, Wright and Walter (1987) pointed out that the initial negative slope of the effective stress vs. the effective plastic strain curve strongly influences
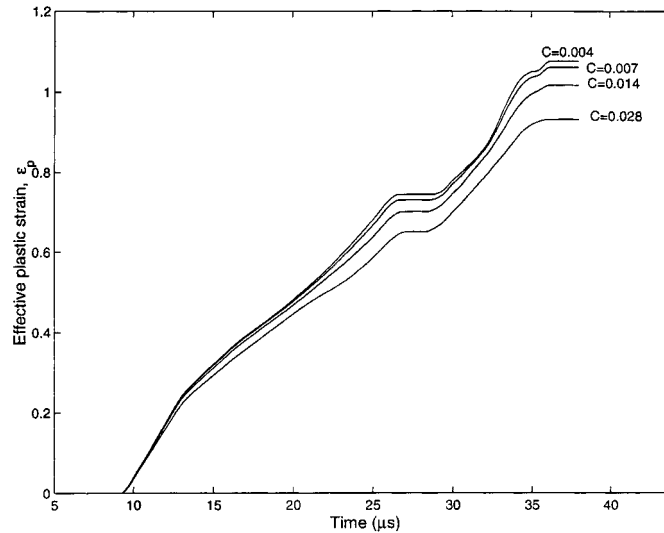
Figure 16. Time history of the evolution of the effective plastic strain in element *E* (see Figure7(b) for its location) for *C* = 0.004, 0.007, 0.014 and 0.028.

the initiation of a shear band. Stevens and Batra (1998) studied the Taylor impact test for a tungsten heavy alloy (WHA) rod, and assumed that the rod was made of either pure tungsten (W), or a homogeneous iron-nickel tungsten (Fe-Ni-W) alloy, or Fe-Ni-W particles randomly interspread among W particles. They found that a shear band formed at the point on the rod's mantle where the mushroomed region transitioned into the straight rod only in the rod with the largest value of the magnitude of the initial negative slope of the effective stress vs. the effective strain curve.

As was noted by Batra and Nechitailo (1997) the computed value of the maximum velocity imparted to the plate particles on the impact face was found to be one-half of the initial velocity of the projectile.

We now discuss results for the prenotched plate with values of variables listed in (16) except for *m* which is set equal to 0.6. This material exhibits enhanced thermal softening and a shear band should initiate when the effective plastic strain slightly exceeds the value at which the effective stress peaks. The impact of the plate by the rod causes a compressive wave to travel into the plate towards the notch-tip. As soon as a wave arrives at the notch-tip, the material there is significantly deformed. The velocity field in the region surrounding the notch-tip, plotted in Figure 4 for two different values of the time reckoned from the instant of impact, shows that initially the material above the upper flat surface of the notch moves rather slowly and that below the lower surface of the notch moves rapidly in the direction of $\mathbf{V}_0$. Material particles near the traction free lower surface of the notch also move upwards due to the Poisson effect. This upward movement of particles essentially subsides once the material near the notch-tip has been plastically deformed; see Figure 4(b). It is clear that the notch-tip has been severely deformed and is no longer circular. The lower surface of the notch close to the notch-tip is displaced upwards by about 0.05 mm while the upper surface has barely moved. The displacement in the direction of $\mathbf{V}_0$ of particles on the lower surface of the notch stretches material lines on the upper curved surface of the notch and induces there a tensile hoop stress. The maximum tensile principal stress occurs at a point, usually a little away

from the notch surface, that in the reference configuration makes an angle of approximately 70° with the notch-axis; the time history of the normalized maximum tensile principal stress, $\sigma_{\max}^t$, at a point in this region is depicted in Figure 5. Note that $\sigma_{\max}^t$ need not always occur at the same material point. However, the maximum effective plastic strain occurs at a point on the notch surface that in the undeformed configuration makes an angle of nearly $-45°$ with the notch-axis. The principal stress with the greatest magnitude in the region surrounding this point is compressive. The time histories of the effective plastic strain, the effective stress, the effective plastic strain-rate and the temperature at this material point are exhibited in Figures 6(a) and 6(b). It is clear that the effective plastic strain-rate, the effective plastic strain and the nondimensional temperature grow rapidly. However, the effective stress first increases extremely fast, and then gradually decreases. The rate of change of these quantities strongly depends upon the notch-tip radius and the thermal softening characteristics of the material of the plate. The effective stress peaks at a rather small value of the effective plastic strain. For a simple shearing problem, Wright and Walter (1987) computed a catastrophic drop in the shear stress within a shear band which was subsequently confirmed by torsional experiments on thin-walled HY-100 steel tubes of Marchand and Duffy (1988). For a simple shearing problem, Batra and Kim (1990) found that the sudden drop in the shear stress caused an elastic unloading wave to emanate out of the shear banded region. However, in plane strain and axisymmetric problems, the rate of drop of the effective stress is generally much less than that in a simple shearing problem because in the former class of problems, the material surrounding the shear banded material constrains the latter from severely deforming; e.g. see Batra and Ko (1993). Figure 7 exhibits the deformed shape of the material adjacent to the notch-tip at times $t = 20,\ 22,\ 24$ and $24.5\,\mu$s. It is evident that the material abutting the bottom surface of the notch-tip is intensely deformed. An opening of the shape of a leaflet develops there which subsequently closes at the notch surface thereby forming an elliptical open area. In order to ensure that this phenomenon is not mesh-dependent, the problem was reanalyzed with the finite element mesh shown in Figure 8. The aspect ratio of elements around the notch-tip for this mesh is close to one. Results obtained with meshes of Figures 2 and 8 were virtually the same.

Time histories, plotted in Figure 6, of different variables at a material point do not clearly indicate when, if at all, a shear band initiates at this material point. Mason et al. (1994) estimated shear strains of 100 percent within a 200–300 μm wide shear band formed in a prenotched plate of C-300 maraging steel. Marchand and Duffy (1988) conducted torsional tests on thin-walled tubes made of a HY-100 steel and measured shear strains of upto 20 within a band. They postulated that a shear band initiates when the torque required to deform the tube suddenly drops. Zhou et al. (1998) assumed a relationship between the effective plastic strain and the effective plastic strain-rate at the tip of a shear band. For a C-300 maraging steel, their relation (5) with values listed in their Table 2 gives the effective plastic strain at the shear band tip to be 0.17 and 0.0636 for effective plastic strain-rates of 4×10^4/s and 4×10^5/s respectively. Batra and Kim (1992) numerically studied the initiation and development of shear bands in simple shearing deformations of twelve materials and concluded that a shear band initiates when the shear stress has dropped to 90 percent of its peak value. However, Deltort (1994) hypothesized that a shear band initiates when the shear stress has dropped to 80 percent of its maximum value. Batra and Rattazzi (1997) studied the initiation and propagation of a shear band in a thick-walled steel tube and investigated the effect of the following four criteria for the initiation of a shear band:

 (i) the effective plastic strain equals 0.5,
 (ii) the effective plastic strain equals 1.0,
(iii) the effective stress has dropped to 90 percent of its peak value, and
(iv) the effective stress has dropped to 80 percent of its maximum value.

As was also found by Batra and Rattazzi (1997) these four definitions of the initiation of a shear band give quite different results for the present problem. We note that Tresca (1878) observed shear bands during the hot forging of a platinum bar and conjectured that the tangential velocity is discontinuous across a shear band. Batra and Ko's (1993) computations showed that this indeed was the case. This criterion for the development of a shear band could not be adopted for the present problem mainly because the band did not propagate far enough from the notch-tip for most cases studied.

We now delineate the effect of different parameters on the time of initiation, t_{is}, of a shear band according to criterion (i). It follows from the results plotted in Figure 6(a) that for an effective plastic strain of 0.5, the effective stress has dropped to 0.85 of the maximum value. Figures 9(a) and 9(b) depict the dependence of t_{is} on different material and geometric parameters, and the impact speed. A four-fold increase in the value of C increases t_{is} by only 6 percent. Values of m, T_m, B, A, V_0 and r_0 strongly influence when a shear band initiates. t_{is} decreases with an increase in V_0 and a decrease in r_0, B, m and T_m. For the three values 0.13, 0.25 and 0.52 of the strain hardening exponent n, the shear band initiates essentially at the same time. Also the length of the projectile had no effect on t_{is}; this agrees with the test observations of Mason et al. (1998). t_{is} increases when A is changed in either direction from the base value. Results could not be satisfactorily computed for $A = 0.39$ GPa because the plate material near the bottom of the projectile/plate impact surface got severely deformed. Even though the data points in Figure 9 have been joined by straight lines, there is no implication that such is indeed the case. The intent is to identify parameters which play a prominent role.

According to criteria (i)–(iv) the time of initiation of a shear band equals 17, 24, 14.5 and 20 μs respectively. As noted earlier, the value of t_{is} depends upon the criterion used. The speed of propagation of a shear band also depends upon the criterion used to define the shear band tip, and was found to be about 50 m/s for most of the cases studied here. Henceforth we use criterion (i) to define a shear band.

Assuming that brittle failure initiates when the maximum tensile principal stress equals twice the yield stress of the material in a quasistatic simple tension or compression test, we have plotted in Figures 9(c) and 9(d) the dependence of the time of initiation of the brittle failure upon different material and geometric parameters. A comparison of these results with those plotted in Figures 9(a) and 9(b) reveals which failure mode will initiate first. It is clear that a material with a smaller value of n will first experience brittle failure and a shear band will first initiate in the material with a higher value of n. As expected, a shear band will first initiate in a material exhibiting increased thermal softening due to lower value of m. The value of T_m does not noticeably change the time of initiation of the brittle failure but significantly affects the time of initiation of a shear band. This can be explained by noting that the temperature rise is very small at points on the upper surface of the notch-tip where brittle failure ensues. However, material points within the shear banded region are significantly heated up (cf. Figure 6(b)) and the material response there is strongly influenced by the value of T_m. For a given temperature rise, a lower value of T_m enhances the thermal softening of the material which results in an earlier initiation of the shear band. The value of the quasistatic

yield stress, A, or the strength of the material has a predominant effect on the failure mode; this agrees with the observations of Mason et al. (1998). An increase in the value of A considerably delays the initiation of a shear band but lowers the time of initiation of the brittle failure. However, higher values of B delay the initiation of both the shear band and the brittle failure. An increase in the value of n has a little effect on the time of initiation of a shear band but noticeably delays the onset of brittle failure. Similarly, an increase in the value of C has a very small effect on the time of initiation of the shear band but considerably decreases the time of initiation of the brittle failure.

Whereas the length of the projectile has virtually no effect on the time of initiation of a shear band, it strongly influences the time of initiation of the brittle failure. For longer projectiles, the brittle failure will first ensue at a point near the upper surface of the notch. The time of initiation of a shear band significantly decreases with an increase in the impact speed. For a projectile speed of 25 m/s, brittle failure will occur first but for projectile speeds, V_0, greater than or equal to 50 m/s, a shear band will initiate first at a point near the notch-tip. For $V_0 = 50$ m/s, a decrease in the notch-tip radius decreases the time of initiation of a shear band and the brittle failure. For $r_0 = 0.05$ and 0.1 mm, a shear band will initiate sooner than the brittle failure.

The foregoing observations on the failure mode depend upon the criteria used to define a shear band and the onset of brittle failure.

We now delineate the effect of different parameters on the deformations of the material adjacent to the notch-tip.

3.1. EFFECT OF THERMAL SOFTENING

Two material parameters, m and T_m, influence the thermal softening of the material.

3.1.1. *Effect of the value of the thermal softening exponent, m*

The effect of decreasing the value of m is to enhance the thermal softening of the material; cf. Figure 3(b). Figure 10 depicts contours of the effective plastic strain for $m = 0.6,\ 0.7,\ 0.8,\ 0.9$ and 1.03 when the maximum effective plastic strain at any point near the notch-tip equals 1.0; the corresponding times are 24.25, 27, 31, 33 and 35 μs respectively. These plots reveal that two shear bands originate from the bottom surface of the deformed notch-tip; one band propagates at about $-10°$ to the notch ligament and the other at $-128°$. As the value of m is increased or the thermal softening effect is decreased, the band propagating at $-128°$ to the notch-axis subsides and only one band propagates at nearly $-10°$ to the notch-axis. Recall that Kalthoff measured the angle between the shear band and the notch-axis to be between $-10°$ and $-15°$. As expected, the time measured from the instant of impact, when the maximum effective plastic strain equals 1.0 increases with an increase in the value of m. The time histories of the effective plastic strain and the effective stress for element E, shown in Figure 7(b), are similar to each other for all values of m considered (e.g. see Figure 6) except that for $m = 0.6$, the effective plastic strain suddenly increases from 1.4 at $t = 27.3$ μs to 2.7 at 27.4 μs. This is due to the severe deformations of the element E. For a fixed value of time t, the radial distance through which a shear band defined by any one of the four aforestated criteria has propagated decreases with an increase in the value of m.
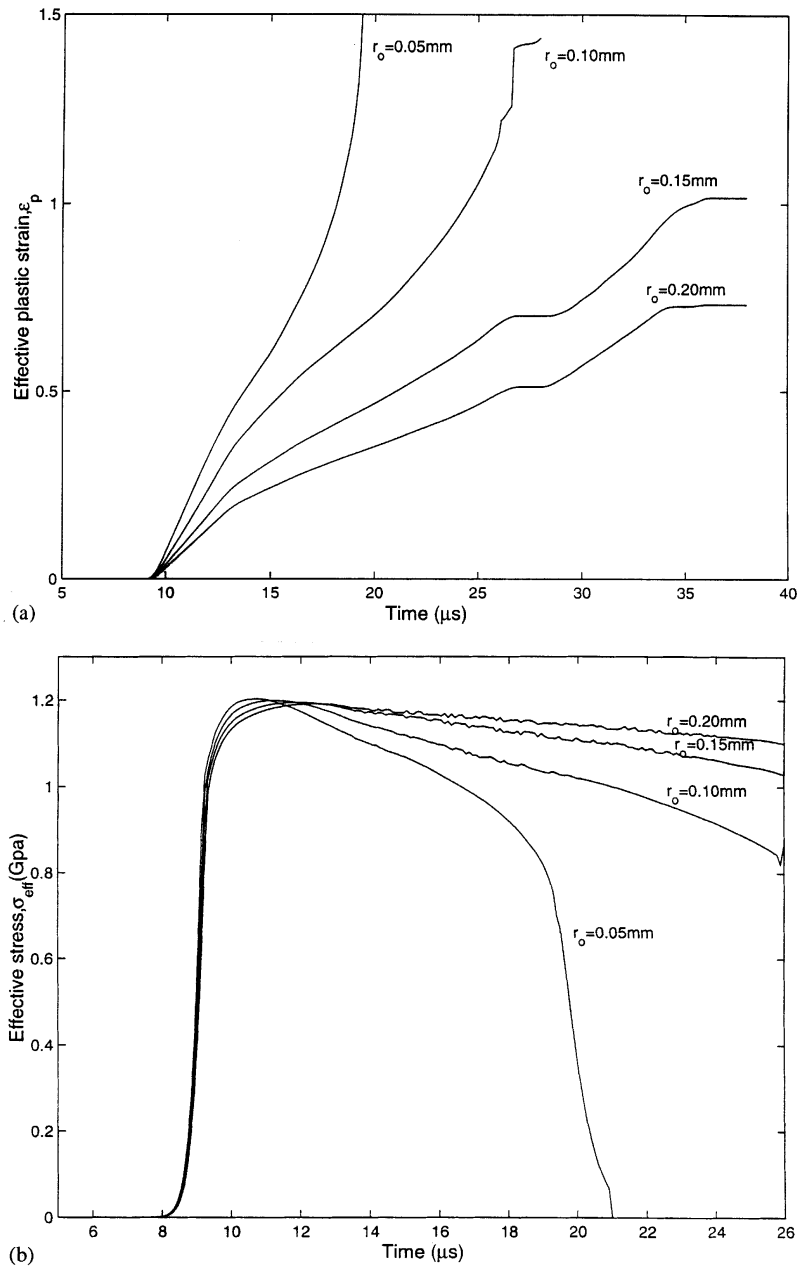
Figure 17(a–b). Time histories of the effective plastic strain and the effective stress for element E (see Figure 7(b) for its location) for different values of the notch-tip radius, r_0.

3.1.2.   *Effect of the value of T_m*

As should be clear from the effective stress vs. the effective plastic strain curves of Figure 3(b), a decrease in the value of T_m enhances the thermal softening effect. Thus the effects of decreasing T_m or m should be similar. Figure 11 depicts contours of the effective plastic strain when the maximum effective plastic strain at any point near the notch-tip equals 1.0;
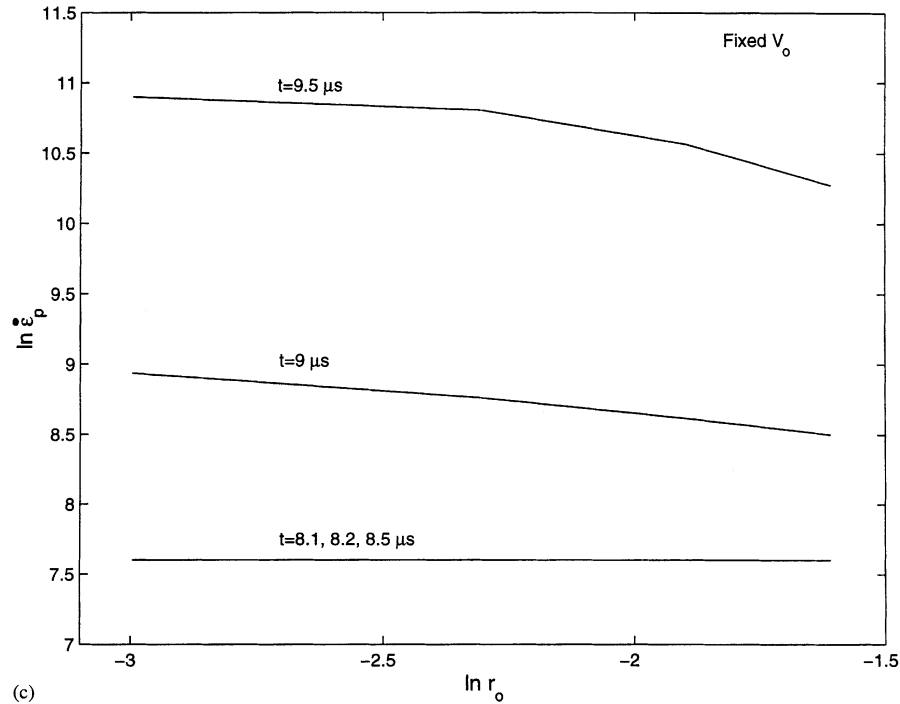
Figure 17(c). Variation of $\ell n \, \dot{\varepsilon}_p$ with $\ell n \, r_0$ at $t = 8.1, \; 9$ and $9.5 \, \mu s$.

the values of the time when this occurs are 24, 28, 35 μs for $T_m = 653, \; 780$ and $1033 \, K$ respectively. A comparison of these plots with those given in Figure 10 reveals that indeed the results are qualitatively similar and shear bands initiate sooner with a decrease in T_m or m. For $T_m = 653 \, K$ the effective plastic strain exceeds 0.5 in the 0.17 mm thick region abutting the notch-surface and extending in the reference configuration from $\theta = -38°$ to $\theta = -90°$ where positive θ is the angle measured counterclockwise from the notch-axis. The thickness or the angular width of this region decreases as one moves away from the notch surface. The speed of the band, defined as a contour of effective plastic strain of 0.5, first increases from about 10 m/s at the instant of initiation to approximately 50 m/s when it has propagated radially through 0.3 mm and then decreases. The width of the band and the radial distance through which it propagates decrease with an increase in the value of T_m. For $T_m = 1413 \, K$, the maximum effective plastic strain never reaches 1.0 in any element around the notch-tip, and for $T_m = 1033 \, K$ the width of the shear banded region (i.e., where the effective plastic strain equals at least 0.5) adjacent to the notch-tip equals 0.14 mm and it extends from $\theta = -27°$ to $\theta = -80°$ in the circumferential direction and 0.1 mm in the radial direction.

3.2. EFFECT OF QUASISTATIC YIELD STRESS, A

The values of the quasistatic yield stress, A, strongly influence the deformations of the material near the notch-tip. Recall that the projectile and the plate are made of the same material. Mason et al.'s (1998) test observations indicate a strong dependence of the shear band propagation
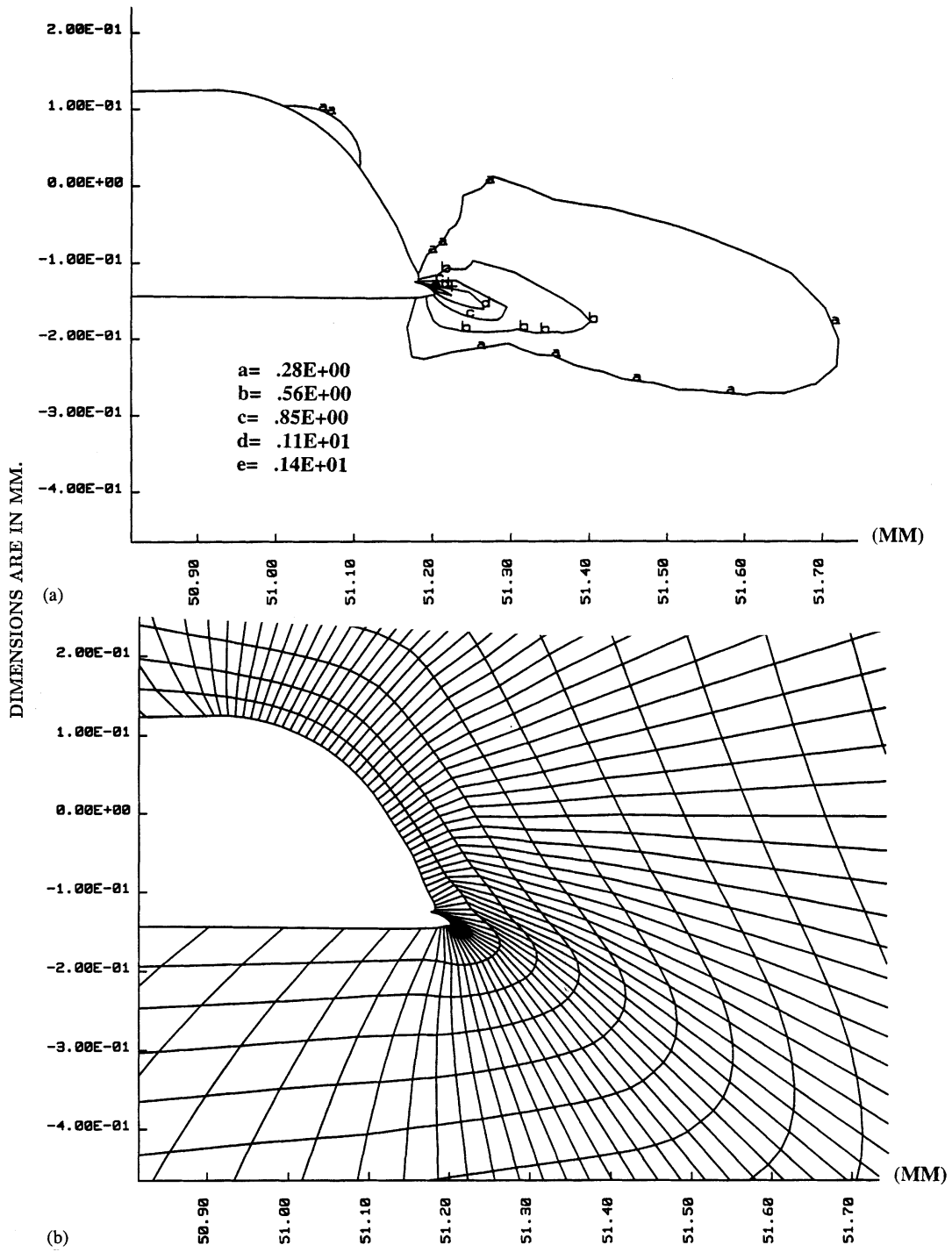
Figure 18. Contours of the effective plastic strain and the deformed mesh at $t = 40\,\mu s$ for the 150 mm long projectile.
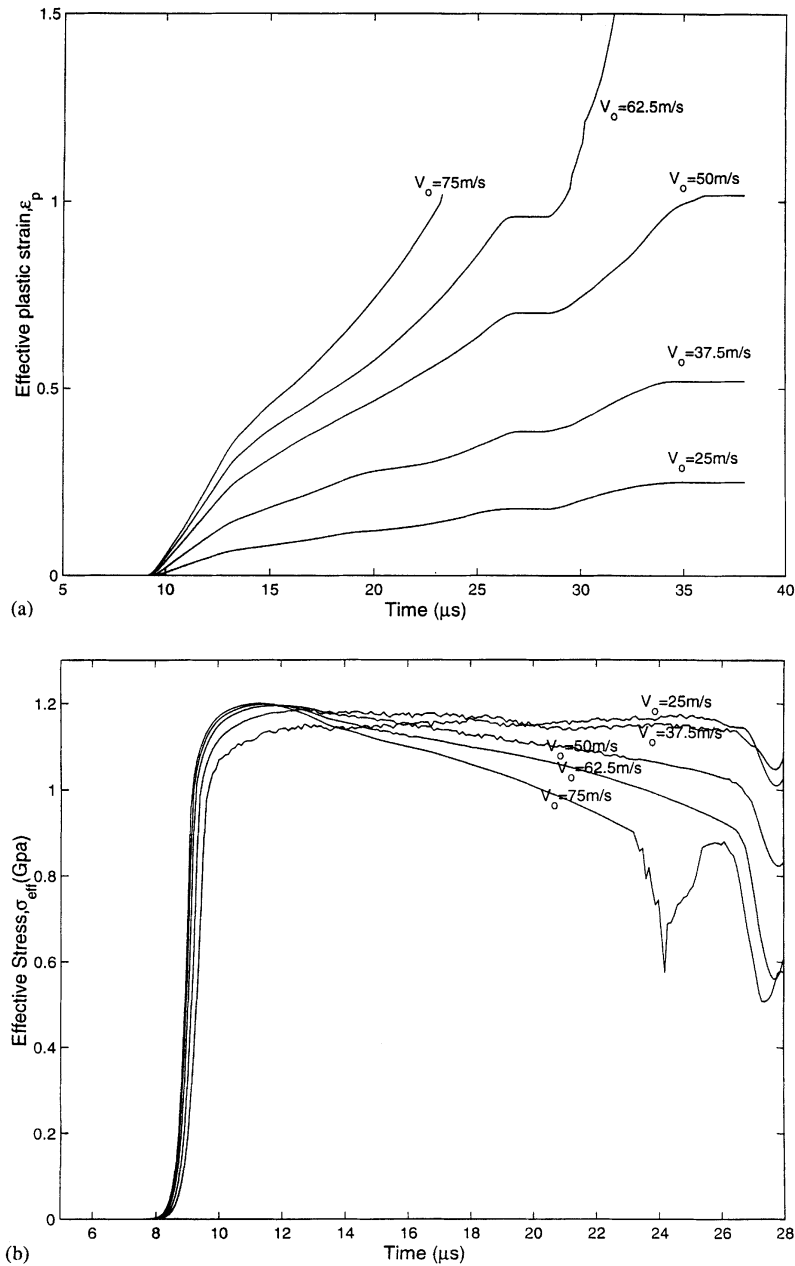
Figure 19(a–b). Time histories of the effective plastic strain and the effective stress for element E (see Figure 7(b) for its location) for different values of the impact speed V_0.

speed and the final length of the band upon the aging condition and hence on the strength of the steel. For four different values of A, Figure 12 exhibits contours of the effective plastic strain when the effective plastic strain at any point near the notch-tip equals 1.0; this happens at $t = 30.75$, 31, 32 and 36 μs for $A = 2.376$, 1.584, 1.18 and 0.63 GPa respectively. Whereas for lower values of A there are two intensely deformed regions originating from the point on
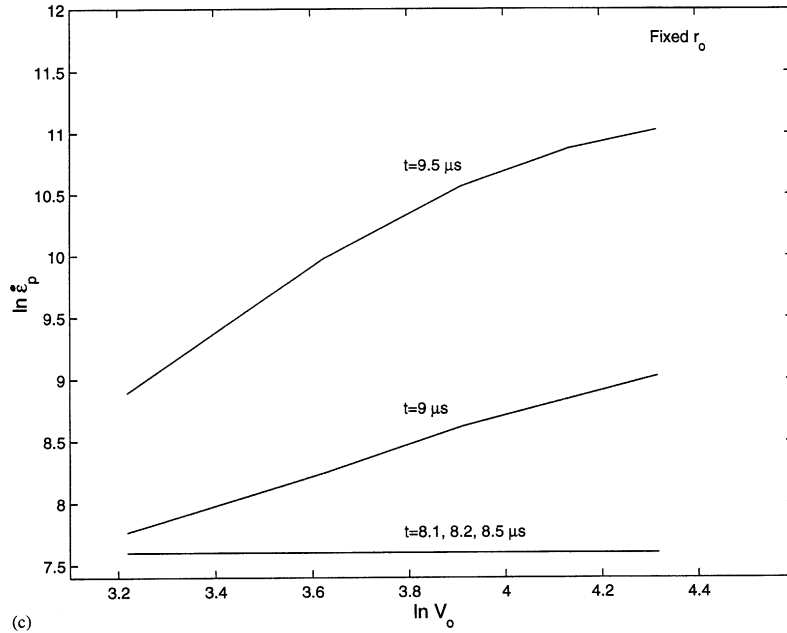
Figure 19(c). Variation of $\ell n\, \dot{\varepsilon}_p$ with $\ell n\, v_0$ at $t = 8.1,\ 9$ and $9.5\,\mu$s.

the bottom surface of the deformed notch-tip, there is only one such region for the highest value 2.376 GPa of A. Note that the value of A determines the strength of a steel. For very high strength steels, only one shear band propagating essentially parallel to the axis of the notch forms. Also, deformations of the material adjacent to the notch-tip are similar to that shown in Figure 7 for low values of A but no leaflet like opening develops for $A = 2.376$ GPa even though the maximum effective plastic strain there exceeds 1.0. Figure 13 depicts at $t = 24\,\mu$s the deformed mesh near the notch surface for $A = 2.376$ GPa and also the velocity field. Whereas for lower values of A the material particles adjacent to the traction free lower surface of the notch move essentially horizontally at $t = 24\,\mu$s, for the higher value of A, their velocity has a small downward component. For $A = 2.376$ GPa the shear band defined as the region in which the effective plastic strain exceeds 0.5 was 71 μm wide near the notch-tip and extended 0.48 mm in the radial direction. The band width near the notch-tip decreased from 150 μm for $A = 0.63$ GPa to 71 μm for $A = 2.376$ GPa.

For $A = 0.39$ GPa, the notch closed near the impacted end at $t = 19\,\mu$s. In order to circumvent this the notch width near the impacted end was increased to 0.5 mm by keeping the lower traction free surface of the notch horizontal and making the upper one inclined to obtain a notch opening of 0.3 mm at a distance of 20 mm from the impacted end. In this case the mesh near the bottom of the target/projectile interface was severely distorted.

3.3. EFFECT OF STRAIN-HARDENING

Two material parameters, B and n, influence the strain hardening of the material; smaller values of n for $\varepsilon_p < 1$ and higher values of B enhance the strain hardening effect of the material. For $\varepsilon_p > 1$, a material with higher value of n will exhibit more strain hardening effect. As pointed out earlier, higher values of B result in larger values of the time, t_{is}, of the initiation of a shear band. Also, only one shear band originates at the notch-tip and propagates

nearly horizontally, i.e., parallel to the axis of the notch. Figure 14 depicts contours of the effective plastic strain and the deformed shape of the notch-tip at $t = 38\,\mu$s for a material with $B = 1.018$ GPa. The maximum effective plastic strain at the notch-tip equals 0.76. It is evident that the surface of the notch-tip is not as severely distorted as for lower values of B, and only a few elements in the region where the deformed notch-tip meets the lower surface of the notch exhibit intense plastic deformations. Similar deformation patterns were observed for a material with $n = 0.13$. We should add that for $B = 0.203$ GPa, a leaflet like opening akin to that exhibited in Figures 7(c) and 7(d) formed. Figure 15 evinces, for four values of B and two values of n, the time history of the temperature in an element abutting the notch surface and situated in the reference configuration on a line that makes an angle of 45° clockwise with the notch-axis. Lower values of B and n result in higher final temperatures at this element. These values of temperatures compare favorably with those experimentally measured by Zhou et al. (1996a).

3.4. EFFECT OF STRAIN-RATE HARDENING

As should be obvious from the plot in Figure 16 of the time history of the evolution of the effective plastic strain at element E for $C = 0.004, 0.007, 0.014$ and 0.028, values of C within the range studied influence a little the initiation of a shear band. Other results such as the deformed surfaces of the notch-tip, the shear band speed, and the velocity field in the deforming region were also essentially unaffected by the value of C.

3.5. EFFECT OF NOTCH-TIP RADIUS, r_0

The maximum tensile principal stress induced at any point near the surface of the notch-tip and normalized by the quasistatic yield stress of the material equals 2.02 for $r_0 = 0.05$ mm, and 2.27 for $r_0 = 0.1, 0.15$ and 0.2 mm. Thus the maximum principal tensile stress is essentially independent of the notch-tip radius; Batra and Nechitailo's (1997) results for larger values of r_0 gave a similar trend. At $t = 18\,\mu$s the deformed surface of the notch-tip for $r_0 = 0.05$ mm looks similar to that shown in Figure 7(c) in the sense that a leaflet like opening develops in the region where the deformed notch surface meets the bottom traction-free surface of the notch. Both the upper and lower traction free surfaces of the notch move upwards, the lower one moves up by 0.043 mm and the upper one by 0.013 mm; thus the gap between these surfaces decreases from 0.1 mm at $t = 0$ to 0.068 mm at $t = 18\,\mu$s. Recall that for $r_0 = 0.15$ mm, the upper traction free surface of the notch scarcely moved. As shown in Figure 9(b) the time of initiation of the shear band, i.e., the time when the maximum effective plastic strain at a point on the notch surface equals 0.5, decreases sharply with a decrease in the notch-tip radius.

For different values of r_0, we have plotted in Figures 17(a) and 17(b) the time-history of the effective plastic strain and the effective stress for element E. For $r_0 = 0.05$ mm, the effective stress drops catastrophically and the effective plastic strain increases immensely at $t \simeq 18\,\mu$s. The drop of the effective stress to zero indicates that the temperature of the material point E has reached the presumed melting temperature of 1033 K. At $t = 18\,\mu$s, a leaflet like opening somewhat similar to that shown in Figure 7(c) developed.

Figure 17(c) depicts the plot of $\ell n\,\dot{\varepsilon}_p$ vs. $\ell n\,r_0$ at $t = 8.1, 9$ and $9.5\,\mu$s, $\dot{\varepsilon}_p$ and r_0 have been normalized by 1/s and 1 mm respectively. Here $\dot{\varepsilon}_p$ equals the effective plastic strain-rate in the element abutting the notch-tip. Assuming that $\dot{\varepsilon}_p\,\alpha\,r_0^{\alpha}$, we conclude from the slopes of the best fit straight lines to the computed values that $\alpha = 0, -0.31$ and -0.43 at $t = 8.1, 9$ and $9.5\,\mu$s respectively. At $t = 8.1\,\mu$s the material near the notch-tip just starts deforming

plastically. Thus the order of the singularity at the notch-tip changes with an increase in the plastic deformation there.

We note that for $r_0 = 0.05$ mm the notch opening near the impacted surface of the plate was increased by keeping the lower notch surface horizontal and making the upper one inclined for about 20 mm. For $t < 18\,\mu s$ the notch surfaces stayed apart but they contacted at $t \simeq 18\,\mu s$ at the point where the upper inclined notch-surface met the lower horizontal notch-surface. It seems that forces at the contact surface had little influence on the deformations near the notch-tip since the material there had already been intensely deformed.

3.6. EFFECT OF PROJECTILE LENGTH

The duration of the loading pulse at the projectile/target interface is directly proportional to the length of the projectile. Whereas for a 75 mm long projectile the maximum effective plastic strain at any point near the notch-tip reached 1.0 at $t = 35\,\mu s$, it equalled 1.7 at $t = 40\,\mu s$ for 112.5 mm and 150 mm long projectiles. For a 150 mm long projectile, contours of the effective plastic strain and the deformed mesh near the notch-tip at $t = 40\,\mu s$ are exhibited in Figure 18. Only one shear band emanates from the point where the deformed notch-tip meets the bottom nearly horizontal surface of the notch and propagates, in the direction of the impact velocity, at an angle of $-10°$ to the horizontal axis. There is no leaflet like open region developed near the bottom of the deformed notch-tip which looks similar to the deformed notch-tip for $A = 2.376$ GPa.

3.7. EFFECT OF IMPACT SPEED, V_0

Figures 19(a) and 19(b) exhibit for element E marked in Figure 7(b) the time histories of the effective plastic strain and the effective stress for different values of the impact speed V_0. For $V_0 = 25$ m/s the maximum effective plastic strain induced at any point near the notch-tip is less than 0.3. The value of the maximum effective plastic strain increases with an increase in the impact speed. For $V_0 \leqslant 25$ m/s there is no shear band formed according to any one of the four aforestated criteria. However, for $V_0 = 25$ m/s, the maximum tensile principal stress equals 2.14 times the quasistatic yield stress, A, of the material. Thus if the brittle failure of the material occurs when the maximum principal tensile stress equals $2A$, then the brittle failure will occur at low impact speeds. At high impact speeds, the maximum effective plastic strain reaches the critical value of 0.5 before the maximum tensile principal stress becomes $2A$, thus a shear band initiates first. Once a material point fails, new surfaces are created and the boundary conditions change; this has not been pursued here. In order to satisfactorily compute results for $V_0 = 75$ m/s, the upper surface of the notch near the impacted end was made inclined as described before.

For low impact speeds, the notch-tip is not intensely deformed and the computed deformed surface of the notch-tip is smooth. For $V_0 = 75$ m/s, a leaflet like opening develops as shown in Figure 7(c) and two shear bands, one at $-10°$ and the other at $-128°$ emanate from the area containing the leaflet.

We have plotted in Figure 19(c) $\ell n\,\dot{\varepsilon}_p$ vs. $\ell n\,V_0$ for three different values of time; $\dot{\varepsilon}_p$ and V_0 have been normalized by 1/s and 1 m/s respectively. Here $\dot{\varepsilon}_p$ equals the effective plastic strain-rate in the element abutting the notch-tip. By fitting straight lines by the least squares method we find that $\dot{\varepsilon}_p \propto V_0^{\beta}$ with $\beta = 0$, 1.16 and 3.42 for $t = 8.1,\ 9$ and $9.5\,\mu s$ respectively. Thus the strain-rate induced at the notch-tip soon after the arrival there of a loading wave is

independent of the speed of the projectile. However, subsequent values of $\dot{\varepsilon}_p$ increase sharply with an increase in V_0.

3.8. PLATE MADE OF A C-300 STEEL

Mason et al. (1994) and Zhou et al. (1996a) tested prenotched plates made of a C-300 steel. Zhou et al. (1996) have given the time histories of the temperature at material points approximately 3 mm and 6 mm from the notch-tip, band speed and the length of a shear band. They modeled the strain and strain-rate hardening of the material by power law type relations and the thermal softening by an exponentially decaying function. Since strain-rate hardening plays a less noticeable role and the strain-hardening in the Johnson–Cook model is analogous to a power law type function, we changed the thermal softening function in eqn. (10) to the one used by Zhou et al. and arrived at

$$\sigma_m = \max[(A + B(\varepsilon_p)^n)(1 + C\ln(\dot{\varepsilon}_p/\dot{\varepsilon}_0^p))(1 - \delta(\exp((T - T_0)/\kappa) - 1)), 0], \qquad (17)$$

where T_0 equals the room temperature. Values of material parameters A, B, n, C, $\dot{\varepsilon}_0$, and κ obtained by fitting curves to their data and used to compute results discussed herein are given below.

$$A = 2\,\text{GPa}, \;\; B = 94.5\,\text{MPa}, \;\; n = 0.2, \;\; C = 0.0165, \;\; T_0 = 293\,\text{K},$$
$$\dot{\varepsilon}_0^p = 1.3 \times 10^{-13}/s, \;\; \kappa = 500\,\text{K}. \qquad (18)$$

Values of geometric and other material parameters are the same as those listed in (16).

For values of material parameters given in (18), $\sigma_m = 0$ when $T = 698\,\text{K}$. Generally $\sigma_m = 0$ for a perfect fluid. Thus the material point defined by (17) and (18) will behave like a perfect fluid for $T \geqslant 698\,\text{K}$. Zhou et al. (1996b, 1998) assumed that it behaves like a viscous fluid when $\varepsilon_p \geqslant 0.17$ and 0.0636 for $\dot{\varepsilon}_p = 4 \times 10^4/s$ and $4 \times 10^5/s$ respectively. We have also computed results with $\kappa = 800\,\text{K}$ which implies that the material point turns into a perfect fluid at $T = 941$ K; the latent heat required to melt a solid material particle has been neglected.

Figure 20 depicts the effective stress vs. the effective plastic strain curves for the C-300 steel with $\kappa = 500\,\text{K}$ and $800\,\text{K}$ obtained by analyzing with DYNA2D a simple shearing problem at a nominal strain-rate of $5 \times 10^4/s$. The thermal softening exhibited by the material defined by (17) and (18) is significantly more than that in the C-300 steel for which the experimental effective stress vs. the effective strain curve is given in Figure 9 of Zhou et al. (1998); it seems that they ignored the effect of thermal softening when fitting a curve to the test values. Here, an initial-boundary-value problem corresponding to simple shearing of a block has been analyzed. For each value of κ, the maximum tensile principal stress induced at any point near the notch-tip equalled 1.9 times the quasistatic yield stress of the material in simple tension or compression. For $\kappa = 500\,\text{K}$ and $800\,\text{K}$ a shear band according to criterion (i) defined above initiated at $t \simeq 20.5$ and $23\,\mu\text{s}$ respectively and propagated into the plate at an average speed of 350 m/s. For the two values of κ we have plotted in Figure 21 the time histories of the effective plastic strain, the effective stress, the effective plastic strain-rate and the normalized temperature for the element E depicted in Figure 7(c). For $\kappa = 500\,\text{K}$ a shear band initiates in element E at $t \simeq 20.5\,\mu\text{s}$ and the temperature there equals 603 K; the material point melts at $t \simeq 22\,\mu\text{s}$. The effective plastic strain-rate, $\dot{\varepsilon}_p$, at the instant of the initiation of the shear band at point E equals $8 \times 10^7/s$. Note that $\dot{\varepsilon}_p = 10^7/s$ when the
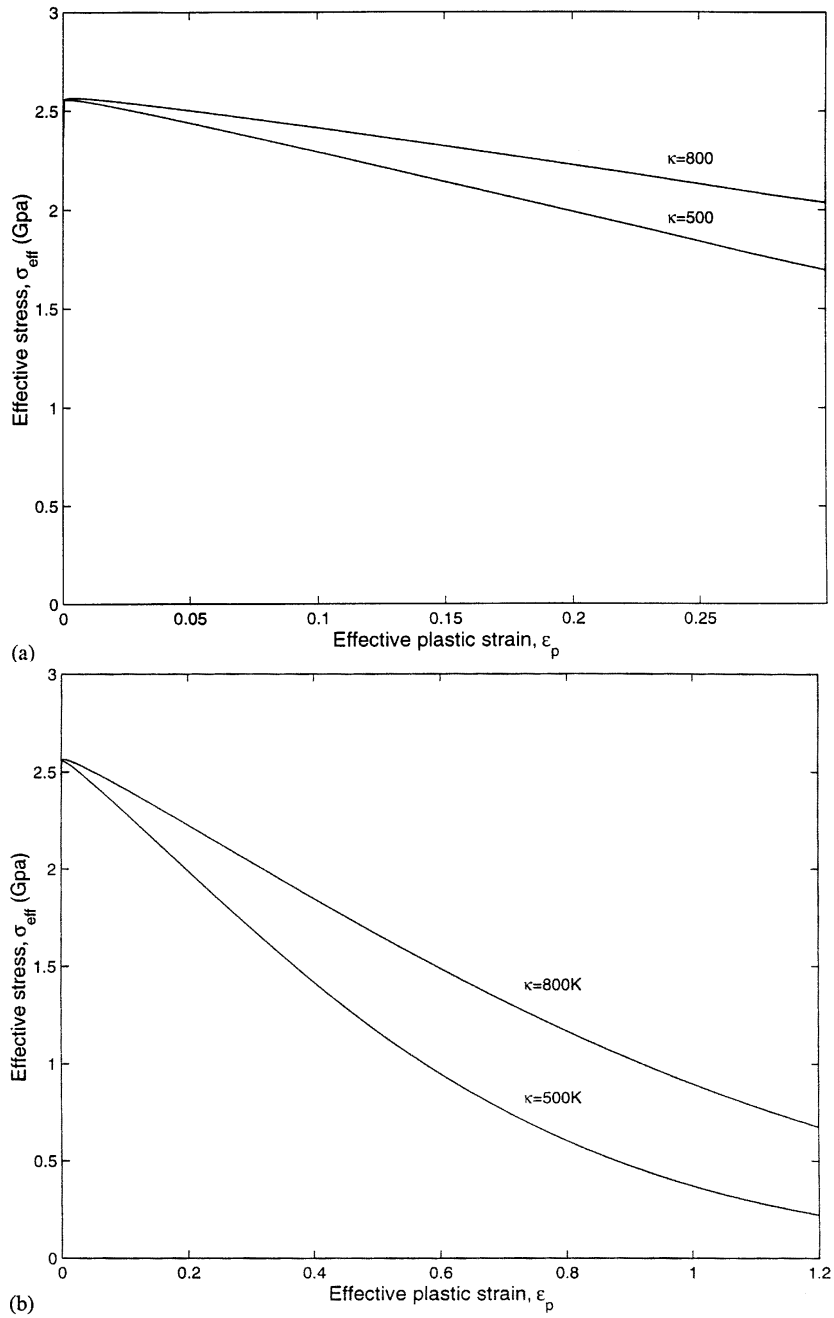
Figure 20. Effective stress vs. effective plastic strain for simple shearing deformations of a C-300 steel deformed at a strain-rate of $5 \times 10^4/\text{s}$.

effective stress at E has the peak value. For $\dot{\varepsilon}_p = 8 \times 10^7/\text{s}$, Zhou et al.'s (1998) Equation (5) implies that the effective plastic strain at the tip of the shear band is 0.04 which is very small. Since the contour of effective plastic strain of 0.04 travels much faster than that of 0.5 (e.g., see Needleman (1989), Zhu and Batra (1991)) the computed band speed will far exceed 350 m/s
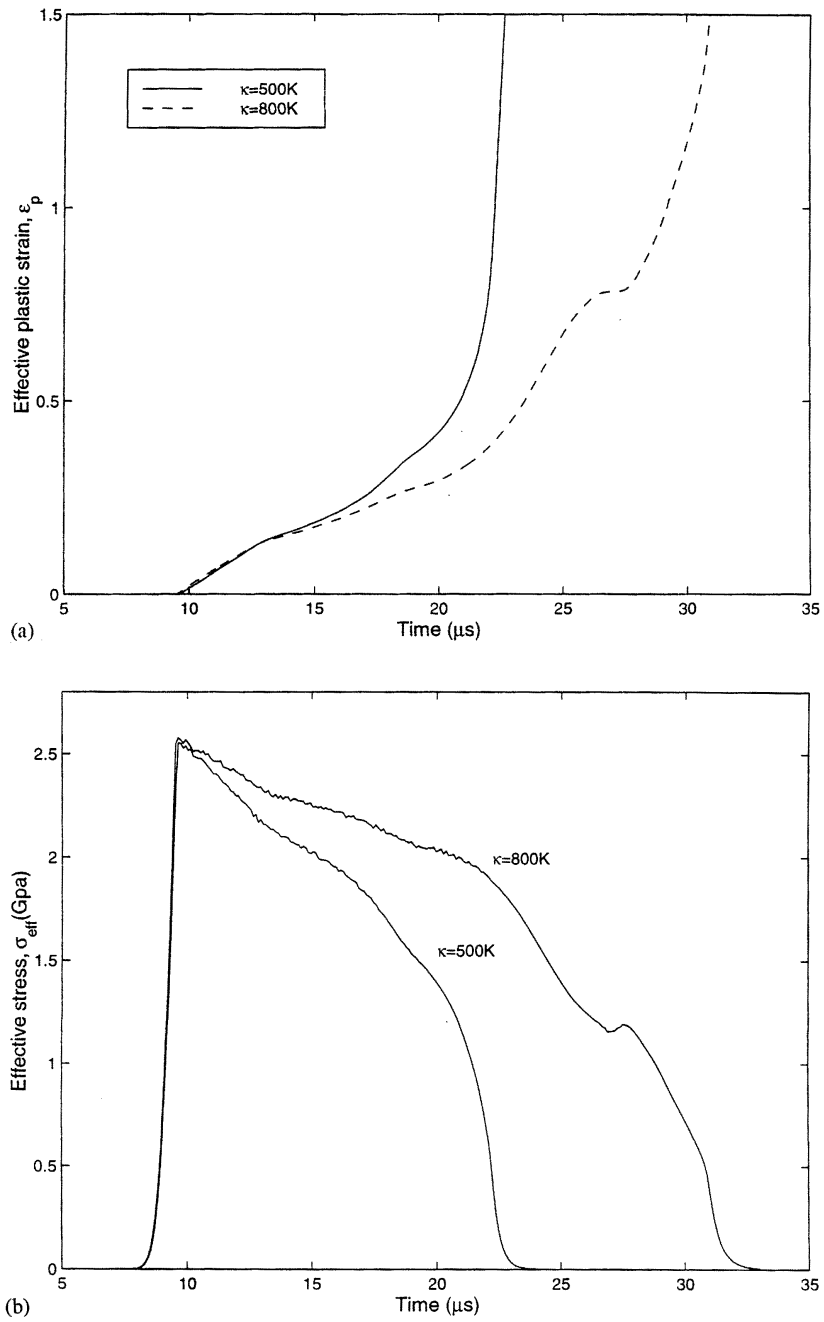
Figure 21a,b.

found here for the contour of $\varepsilon_p = 0.5$. Figure 22 shows for $\kappa = 500\,\text{K}$ the deformed mesh and contours of the effective plastic strain at $t = 22.2\,\mu\text{s}$. Only a small amount of material near the bottom of the notch-tip is intensely deformed and the contour of the effective plastic strain of 0.17 has propagated to a point 0.5 mm from the notch-tip. Results for $\kappa = 800\,\text{K}$ are similar to those for $\kappa = 500\,\text{K}$ except that the initiation of the shear band is delayed a little.
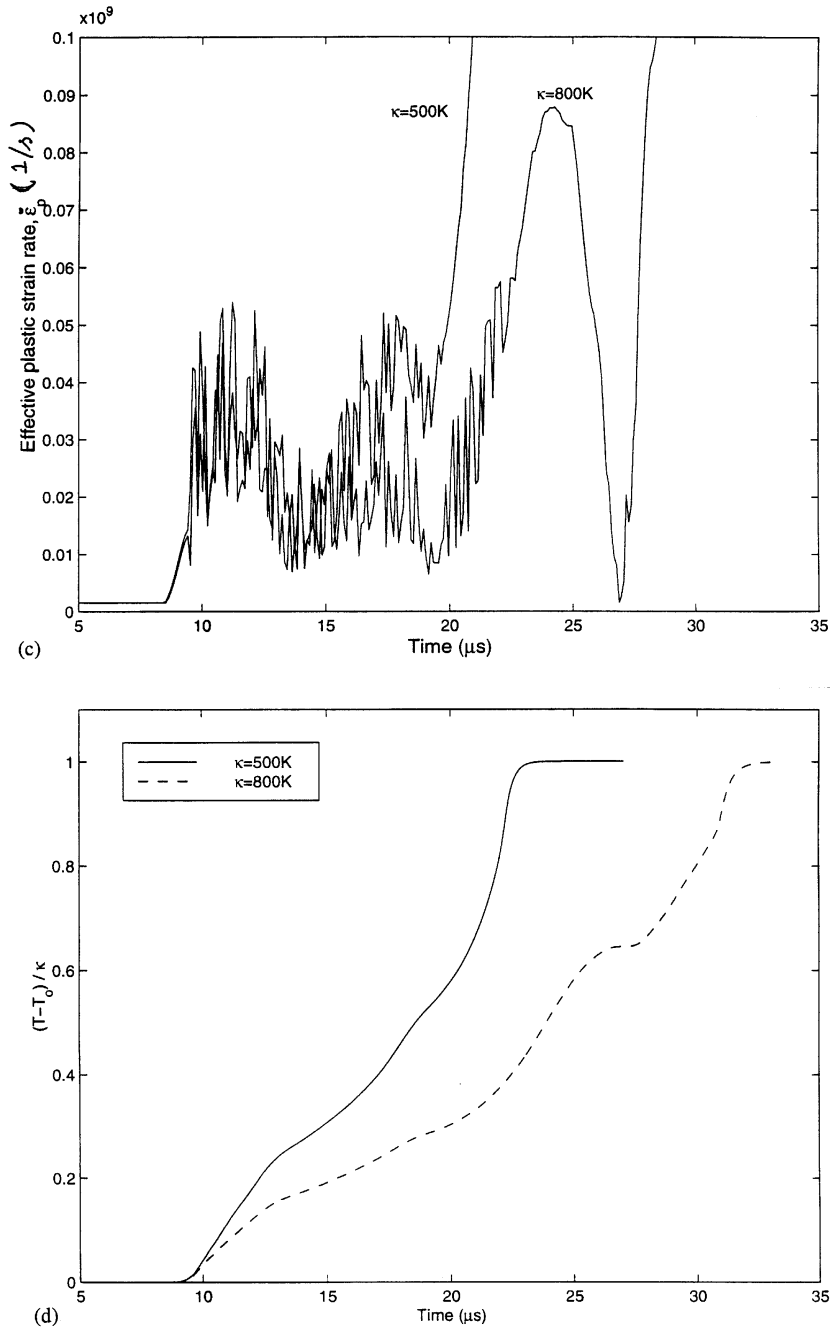
Figure 21. Time histories of the effective stress, effective plastic strain, effective plastic strain-rate and the nondimensional temperature for element E (see Figure 7(b) for its location).

The computed value of the temperature in element E is comparable to that measured by Zhou et al. (1998). However, our computations could not be carried further in time because of the excessive distortions of the elements surrounding the element E. Zhou et al. (1998, 1996b) have not elaborated upon the technique, if any, employed to overcome the severe distortion of elements containing the failed material.
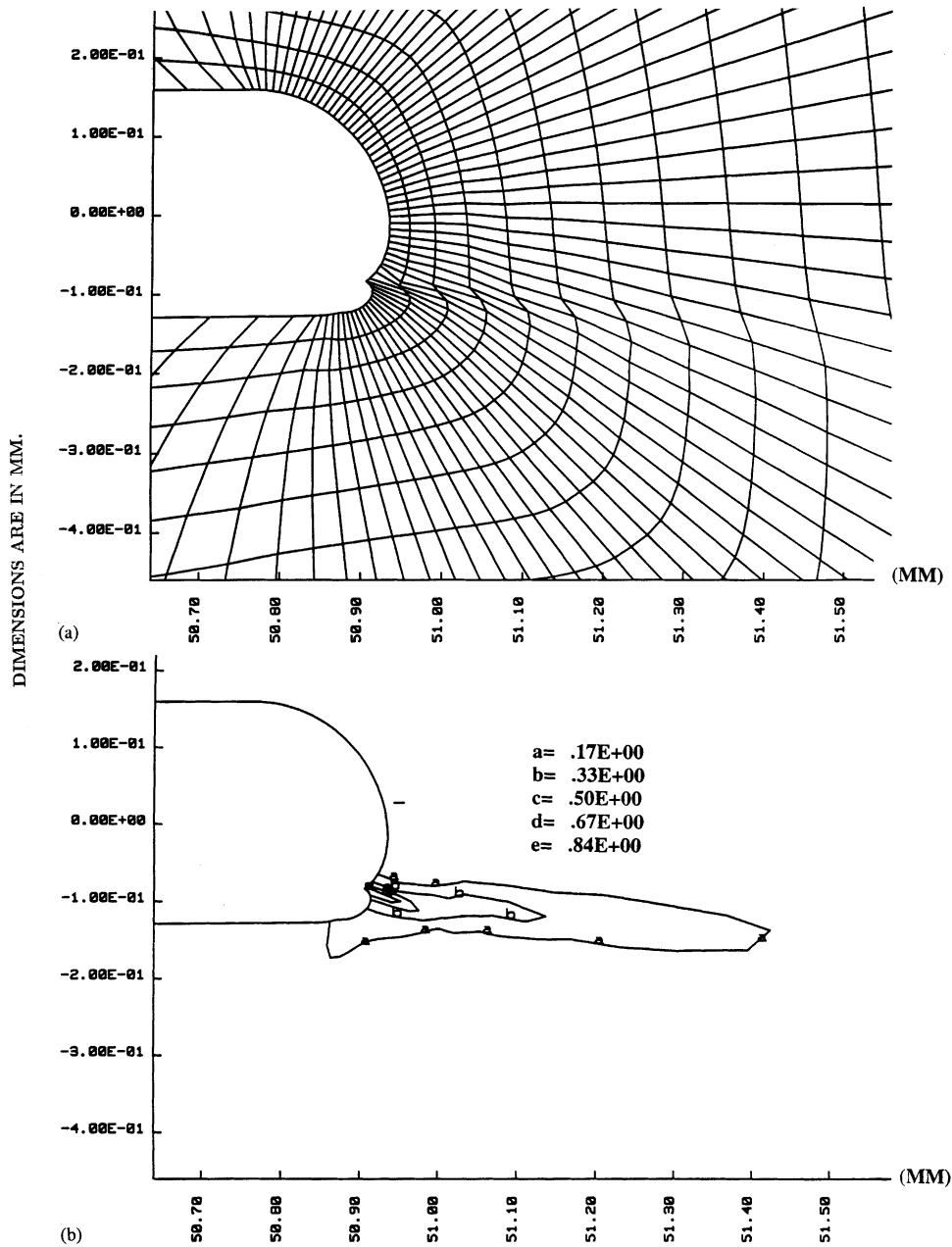
Figure 22. The deformed mesh near the notch-tip and contours of the effective plastic strain for $\kappa = 500$ K at $t = 22.2 \,\mu$s.

Mason et al. (1994) have estimated the shear band speed and the time of initiation, t_{is}, to be 320 m/s and 26 μs respectively. Zhou et al. (1996a) measured the maximum shear band speed to be 2000 m/s in the same C-300 steel. For $\kappa = 500$ K and 800 K, our computed values are $t_{is} = 20.5$ and 23 μs respectively, and the average shear band speed for each value of κ equals 350 m/s.

4. Conclusions

We have analyzed finite plane strain transient deformations in a prenotched plate impacted on the side by a projectile moving parallel to the axis of the notch. The projectile and the plate are assumed to be made of the same material which exhibits strain hardening, strain-rate hardening and thermal softening. The thermoviscoplastic response of the material is modeled by the Johnson–Cook relation. The deformations are assumed to be locally adiabatic and no failure criterion is included. The problem is analyzed for several values of the material and geometric parameters by using the large scale explicit finite element code DYNA2D. For one set of material and geometric parameters, results computed with four different reasonably fine finite element meshes were found to be virtually identical to each other. Results presented in this paper and the conclusions drawn are based on the finest finite element mesh used that had 60 elements around the notch tip. For a notch-tip radius of 0.15 mm, the size of the elements abutting the notch-tip surface equalled $7.85\,\mu$m $\times$ $23.6\,\mu$m.

For all of the cases analyzed, the bottom surface of the notch moves upwards and the upper surface essentially stays stationary except when the notch-tip radius equals 0.05 mm. For the latter case both surfaces move upwards, however the lower one moves by a larger amount than the upper one with the result that the notch opening is decreased as also happens for other problems studied. The lower notch surface is also displaced in the direction of the velocity of the projectile, the notch tip is deformed and line elements near the upper part of the notch surface are stretched. The maximum principal stress is tensile near this part of the notch tip and compressive near the bottom of the deformed notch-tip. However, the maximum effective plastic strain occurs near the bottom of the deformed notch-tip.

It is found that for strongly strain-hardening or high strength (very high values of the yield stress in a quasistatic simple tension or compression test) steels, a shear band initiates from the bottom of the deformed notch-tip and propagates in the direction of the impact velocity at an angle of about $-10°$ with the axis of the notch. The maximum computed shear band speed equals approximately 100 m/s. However, for moderate strength steels, a leaflet like opening develops near the bottom of the deformed surface of the notch tip, and two shear bands – one at $-10°$ and the other at $-128°$ to the notch-axis propagate into the plate material.

For all values of the material and geometric parameters considered with the Johnson–Cook model the maximum tensile principal stress equals about 2.2 times the yield stress of the material in a quasistatic simple tension or compression test. For impact speeds below approximately 30 m/s, the maximum effective plastic strain induced is less than 0.4. With the assumptions that a shear band initiates when the effective plastic strain equals at least 0.5 and the brittle failure occurs when the maximum tensile principal stress equals twice the quasistatic yield stress of the material, brittle failure will occur at low values of the impact speed and a ductile failure at high impact speeds in conformity with the observations of Kalthoff. We note that in problems where the computed maximum effective plastic strain exceeded 0.5, it occured before the maximum tensile principal stress attained its critical value implying thereby that a shear band initiated first.

The initial plastic strain-rate at the notch-tip at $t = 8.1\,\mu$s when a loading wave arrives there is independent of V_0 and r_0, that at $t = 9\,\mu$s and $9.5\,\mu$s is proportional to $V_0^{1.16}/r_0^{0.31}$ and $V_0^{3.42}/r_0^{0.43}$ which differ from the $V_0/r_0^{0.5}$ asserted by Kalthoff. The exponents of V_0 and r_0 will very likely depend upon the constitutive relation employed to model the thermoviscoplastic response of the material.

We have also investigated the dynamic deformations of a prenotched plate made of a C-300 steel modeled by the modified Johnson–Cook relation with the thermal softening function replaced by an exponential one proposed by Zhou et al. (1996b). With the material parameters obtained by fitting curves to Zhou et al.'s data, the average shear band speed was found to be 350 m/s and the temperature rise at the initiation of a shear band to be 305°C. The maximum tensile principal stress equalled 1.9 times the yield stress of the material in a quasistatic simple tension or compression test.

Acknowledgement

References

Batra, R.C. and Jayachandran, R. (1992). Effect of constitutive models on steady state axisymmetric deformations of thermo-elastic-viscoplastic targets. *International Journal of Impact Engineering* **12**, 209–226.

Batra, R.C. and Kim, C.H. (1990a). Adiabatic shear banding in elastic-viscoplastic nonpolar and dipolar materials. *International Journal of Plasticity* **6**, 127–141.

Batra, R.C. and Kim, C.H. (1990b). Effect of viscoplastic flow rules on the initiation and growth of shear bands at high strain rates. *Journal of the Mechanics and Physics of Solids* **38**, 859–874.

Batra, R.C. and Kim, C.H. (1992). Analysis of shear bands in twelve materials. *International Journal of Plasticity* **8**, 425–452.

Batra, R.C. and Ko, K.I. (1993). Analysis of shear bands in dynamic axisymmetric compression of a thermoviscoplastic cylinder. *International Journal of Engineering Science* **31**, 529–547.

Batra, R.C. and Nechitailo, N.V. (1997). Analysis of failure modes in impulsively loaded pre-notched steel plates. *International Journal of Plasticity* **13**, 291–308.

Batra, R.C. and Rattazzi, D. (1997). Adiabatic shear banding in a thick-walled steel tube. *Computational Mechanics* **20**, 412–426.

Deltort, B. (1994). Experimental and numerical aspects of adiabatic shear in a 4340 steel. *Journal de Physique* Colloque C8 **4**, 447–452.

Farren, W.S. and Taylor, G.I. (1925). The heat developed during plastic extrusion of metal. *Proceedings of the Royal Society* **A207**, 422–426.

Johnson, G.R. and Cook, W.H. (1983). A constitutive model and data for metals subjected to large strains, high strain rates and high temperatures. *Proceedings of the 7th International Symposium Ballistics*, The Hague, The Netherlands, 541–548.

Kalthoff, J.F. (1987). Shadow optical analysis of dynamic shear fracture. SPIE, Vol. 1814, *Photomechanics and Speckle Meterology*, 531–538.

Kalthoff, J.F. and Winkler, S. (1987). Failure mode transition at high rates of shear loading. *Impact Loading and Dynamic Behavior of Materials*, (Edited by C.Y. Chiem et al.), Informationsgesellaschaft Verlag Bremen, 185–195.

Klepaczko, J.R., Lipinski, P. and Molinari, A. (1987). An analysis of the thermoplastic catastrophic shear in some metals. *Proceedings of International Conference on Impact Loading and Dynamic Behavior of Materials* (Edited by C.Y. Chiem et al.), Informationsgesellaschaft Verlag Bremen, 695–794.

Lee, Y.J. and Freund, L.B. (1990). Fracture initiation due to asymmetric impact loading of an edge cracked plate. *Journal of Applied Mechanics* **57**, 104–111.

Marchand, A. and Duffy, J. (1988). An experimental study of the formation process of adiabatic shear bands in a structural steel. *Journal of the Mechanics and Physics of Solids* **36**, 251–283.

Mason, J.J., Rosakis, A.J. and Ravichandran, G. (1994a). Full field measurements of the dynamic deformation field around a growing adiabatic shear band tip of a dynamically loaded crack or notch. *Journal of the Mechanics and Physics of Solids* **42**, 1679–1697.

Mason, J.J., Rosakis, A.J. and Ravichandran, G. (1994b). On the strain and strain-rate dependence of the fraction of plastic work converted to heat: an experimental study using high speed infrared detectors and Kolsky bar. *Mechanics of Materials* **17**, 135–150.

Mason, J.J., Zimmerman, J.A. and Roessig, K.M. (1998). The effects of aging condition on shear localization from the tip of a notch in a maraging steel. *Journal of Materials Science* **33**, 1451–1459.

Needleman, A. (1989). Dynamic shear band in plane strain. *Journal of Applied Mechanics* **56**, 1–8.

Needleman, A. and Tvergaard, V. (1995). Analysis of brittle-ductile transition under dynamic shear loading. *International Journal of Solids and Structures*. **44**, 2571–2590.

Rajendran, A.M. (1992). High strain-rate behavior of metals, ceramics and concrete. Report No. WL-TR-92-4006, Wright-Patterson Air Force Base.

Stevens J.B. and Batra, R.C. (1998). Adiabatic shear bands in the Taylor impact test for a WHA rod. *International Journal of Plasticity*. **14**, 841–854.

Sulijoadikusumo, A.V. and Dillon, O.W., Jr. (1979). Temperature distribution for steady axisymmetric extrusion with an application to Ti-6Al-4V, Part I. *Journal of Thermal Stresses* **2**, 97.

Tresca, H. (1878). On further application of the flow of solids. *Proceedings of the Institution of Mechanical Engineers* **30**, 301–345.

Whirley, R.G., Engelmann, B.E. and Hallquist, J.O. (1992). DYNA2D, A nonlinear, explicit, two-dimensional finite element code for solid mechanics, user manual. *Lawrence Livermore National Laboratory Report*, UCRL-MA-110630.

Wright, T.W. and Walter, J.W. (1987). On stress collapse in adiabatic shear bands. *Journal of the Mechanics and Physics of Solids* **35**, 701–720.

Zhou, M., Rosakis, A.J. and Ravichandran, G. (1996a). Dynamically propagating shear bands in prenotched plates: I – Experimental investigations of temperature signatures and propagating speed. *Journal of the Mechanics and Physics of Solids* **44**, 981–1006.

Zhou, M., Rosakis, A.J. and Ravichandran, G. (1996b). Dynamically propagating shear bands in prenotched plates: II – Finite element simulations. *Journal of the Mechanics and Physics of Solids* **44**, 1007–1032.

Zhou, M., Rosakis, A.J. and Ravichandran, G. (1998). On the growth of shear bands and failure mode transition in prenotched plates: A comparison of singly and doubly notched specimens. *International Journal of Plasticity* **14**, 435–451.

Zhu, Z.G. and Batra, R.C. (1991). Shear band development in a thermally softening viscoplastic body. *Computers and Structures* **39**, 459–472.